OPTIMIZATION OF PROCESS PARAMETERS OF DRY ELECTRIC DISCHARGE MACHINING

A MAJOR PROJECT REPORT

SUBMITTED AS PARTIAL FULFILMENT OF THE

REQUIREMENT FOR THE AWARD OF DEGREE OF

MASTER OF ENGINEERING

IN

PRODUCTION ENGINEERING

SUBMITTED BY

SUNILKUMAR PATIL

(UNIVERSITY ROLL NO. 10065)

UNDER THE GUIDANCE OF

DR. R. S. MISHRA

DEPARTMENT OF MECHANICAL & PRODUCTION ENGINEERING
DELHI COLLEGE OF ENGINEERING, UNIVERSITY OF DELHI, DELHI-110042. (SESSION 2010-11)

CANDIDATE DECLARATION

I, SUNILKUMAR PATIL, hereby certify that the work which is being presented in the thesis entitled "**OPTIMIZATION OF PROCESS PARAMETERS OF DRY ELECTRIC DISCHARGE MACHINING.**" in the partial fulfillment of requirement for the award of degree of MASTER OF ENGINEERING submitted in the department of Mechanical Engineering at DELHI COLLEGE OF ENGINEERING under UNIVERSITY OF DELHI, DELHI, is an authentic record of my own work carried out during a period of July 2010 to July 2011, under the supervision of Dr. R. S. MISHRA Professor in Department of Mechanical Engineering. The matter presented in this thesis has not been submitted in any other University/Institute for the award of any degree.

(SUNILKUMAR PATIL)

University Roll No. 10065

This is to certify that the above statement made by the candidate is true to the best of my knowledge.

DR. R. S. MISHRA

(Professor)

Department of Mechanical Engineering

Delhi College of Engineering, Delhi-110042 (INDIA)

ACKNOWLEDGEMENT

I wish to acknowledge my profound sense of gratitude to my project guide Dr. R. S. Mishra, Professor, Department of Production and Industrial Engineering, Delhi college of Engineering, Delhi for his remarkable guidance and many valuable ideas during the preparation of this project. Indeed it was a matter of great felicity and privilege for me to work under his aegis was express my thankfulness to him for his dedicated inspiration, lively interest and patience through my errors with which it would have being impossible to bring the project near to completion.

I wish to extend my hearty thanks to Dr. Suhas Deshmukh & Prof. S.S. Mullik, Mechanical Department at Sihgad Institute of technology, Pune who helped me in this project work. I would like to thank Prof. Sukhvinder Singh BVCOE, New Delhi for his valuable and timely inputs. Also the staff of workshop for their useful contribution.

I wish to extend my hearty thanks to all the staff of the department who directly and indirectly helped me in this project work.

And lastly I express sincere gratitude to Prof. B. D. Pathak HOD, Department of Mechanical Engineering, and Prof. S. K. Garg, HOD, Training and Placement with whose blessing this project was completed.

SUNILKUMAR PATIL

University Roll No.10065

Department of Production and Industrial Engineering.

Delhi College of Engineering, NewDelhi. 2008-2011.

CHAPTER 1

INTRODUCTION

1.1 Introduction

Different non-traditional machining techniques are increasingly employed to manufacture different high quality industrial components. Nontraditional machining processes are necessary for machining of such materials. Among the nontraditional methods of machining processes, electrical discharge machining (EDM) has drawn a great deal of attention because of its broad industrial applications including different dies and tools [1]. Electrical Discharge Machining (EDM) is one such process which is widely used to machine electrically conductive materials. EDM is a thermo-electric process in which material removal takes place through the process of controlled spark generation. In this process material is removed by controlled erosion through a series of electric sparks between the tool (electrode) and the work piece. The thermal energy of the sparks leads to intense heat conditions on the work piece causing melting and vaporizing of work piece material [2]. Due to the high temperature of the sparks, not only work material is melted and vaporized, but the electrode material is also melted and vaporized, which is known as electrode wear (EW). Like other machining processes, the quality of machined parts in EDM is significantly affected by input parameters [3, 4]. This is one of the most popular non-traditional machining processes being used today in the industry. EDM is commonly used in mold and die making industry and in manufacturing automotive, aerospace and surgical components. Since there is no mechanical contact between the tool and the work-piece, thin and fragile components can be machined without the risk of damage.

1.2 Electric Discharge Machining

Electric discharge machining is a thermo-electric non-traditional machining process. Material is removed from the work-piece through localized melting and vaporization of material. Electric sparks are generated between two electrodes when the electrodes are held at a small distance from each other in a dielectric medium and a high potential difference is applied across them. Localized

regions of high temperatures are formed due to the sparks occurring between the two electrode surfaces. Work-piece material in this localized zone melts and vaporizes. Most of the molten and vaporized material is carried away from the inter-electrode gap by the dielectric flow in the form of debris particles. To prevent excessive heating, electric power is supplied in the form of short pulses. Spark occurs wherever the gap between the tool and the work-piece surface is smallest. After material is removed due to a spark, this gap increases and the location of the next spark shifts to a different point on the work-piece surface. In this way several sparks occur at various locations over the entire surface of the work-piece corresponding to the work-piece-tool gap. Because of the material removal due to sparks, after some time a uniform gap distance is formed throughout the gap between the tool and the work-piece. Thus, a replica of the tool surface shape is formed on the work-piece as shown in Figure 1.1. If the tool is held stationary, machining would stop at this stage. However if the tool is fed continuously towards the work-piece then the process is repeated and more material is removed. The tool is fed until the required depth of cut is achieved. Finally, a cavity corresponding to replica of the tool shape is formed on the work-piece.

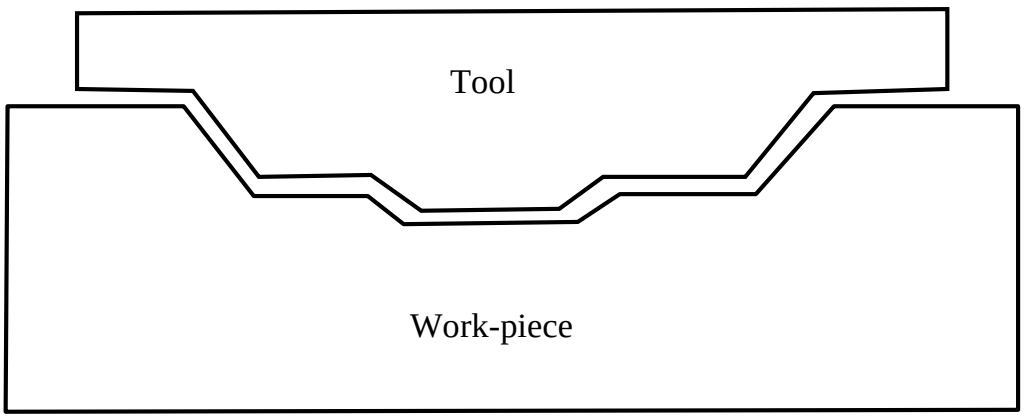

Figure 1.1: Tool Shape and Corresponding cavity formed on work-piece after EDM operation

The schematic of an EDM machine tool is shown in Figure 1.2. The tool and the work-piece form the two conductive electrodes in the electric circuit. Pulsed power is supplied to the electrodes from a separate power supply unit. The appropriate feed motion of the tool towards the work piece is generally provided for maintaining a constant gap distance between the tool and the work-

piece during machining. This is performed by either a servo motor control or stepper motor control of the tool holder. As material gets removed from the work-piece, the tool is moved downward towards the work-piece to maintain a constant inter-electrode gap. The tool and the work-piece are plunged in a dielectric tank and flushing arrangements are made for the proper flow of dielectric in the inter-electrode gap. Typically in oil die-sinking EDM, pulsed DC power supply is used where the tool is connected to the negative terminal and the work-piece is connected to the positive terminal. The pulse frequency may vary from a few kHz to several MHz. The inter-electrode gap is in the range of a few tens of micro meter to a few hundred micrometer. Material removal rates of up to 300 mm3/min can be achieved during EDM. The surface finish (Ra value) can be as high as 50 µm during rough machining and even less than 1 µm during finish machining.

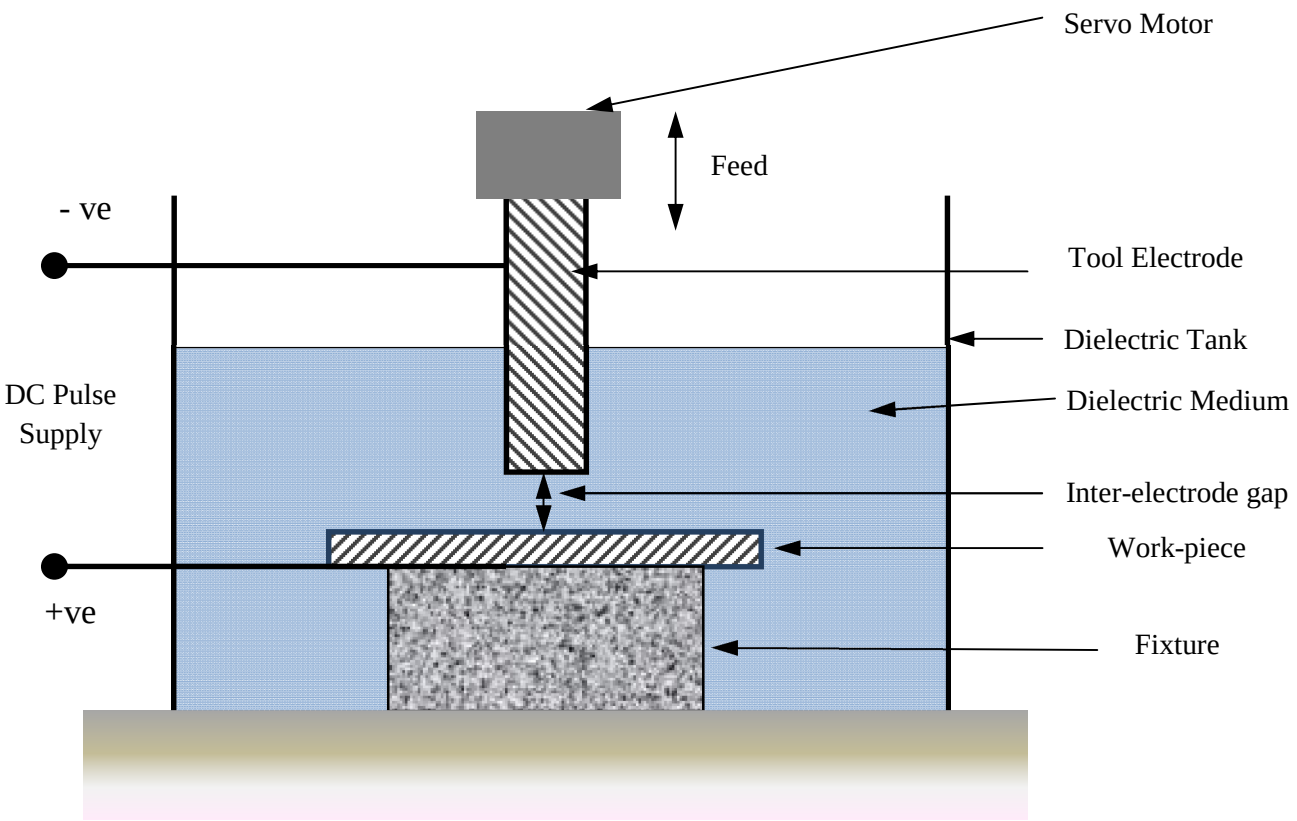

Figure 1.2: Schematic of an Electric Discharge Machining (EDM) Machine Tool

1.3 Dry Electric Discharge Machining

Dry Electric Discharge machining (dry EDM) is a modification of the oil EDM process in which the liquid dielectric is replaced by a gaseous dielectric. High velocity gas flowing through the tool electrode into the inter-electrode gap substitutes the liquid dielectric. The flow of high velocity gas into the gap facilitates removal of debris and prevents excessive heating of the tool and work-piece at the discharge spots. Providing rotation or planetary motion to the tool has been found to be essential for maintaining the stability of the dry EDM process. The dry EDM process schematic is shown in Figure 1.3. Tubular tools are used and as the tool rotates, high velocity gas is supplied through it into the discharge gap. Gas in the gap plays the role of the dielectric medium required for electric discharge. Also, continuous flow of fresh gas into the gap forces debris particles away from the gap. Tool rotation during machining not only facilitates flushing but also improves the process stability by reducing arcing between the electrodes

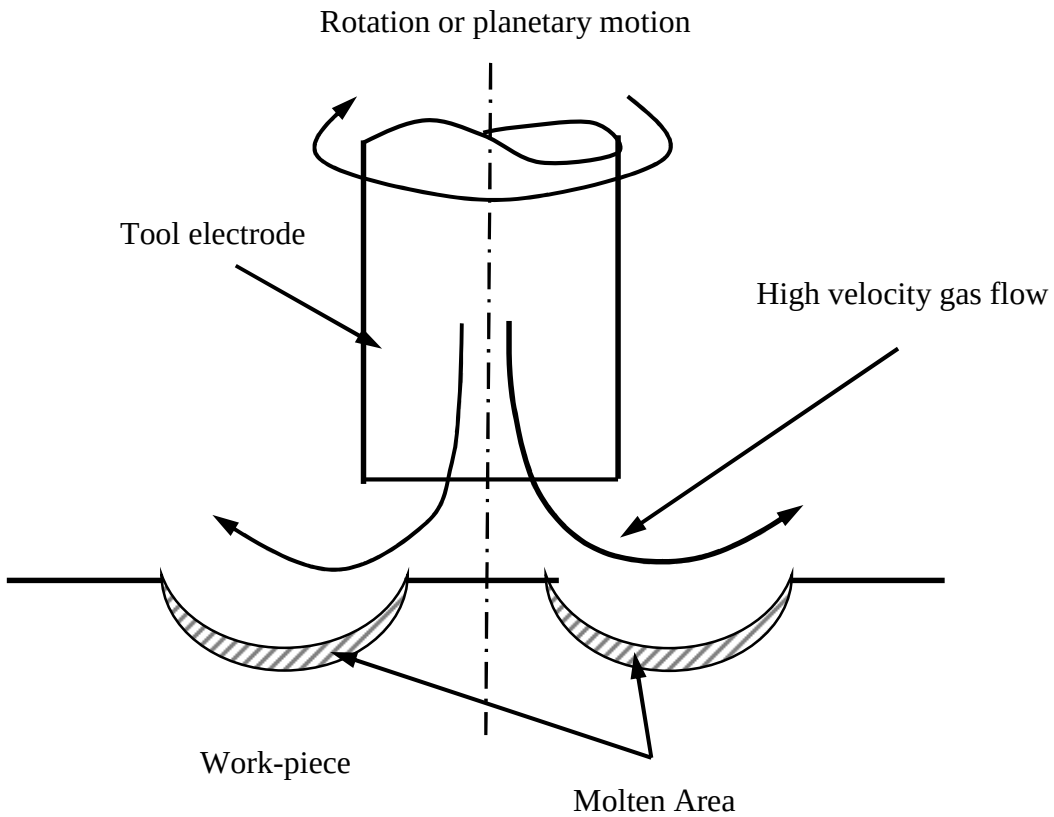

Figure 1.3 : Schematic of Dry EDM Process

Dry EDM is an environment-friendly EDM technique because of the absence of mineral oil-based liquid dielectric. Environmentally harmful oil-based dielectric wastes are not produced in dry EDM. Also, the process does not pose a health hazard since toxic fumes are not generated during machining. Additionally, absence of mineral oil-based dielectrics drastically reduces fire hazards during the process.

1.4 Wire Electric Discharge Machining

The WEDM machine tool comprises of a main worktable (X-Y) on which the work piece is clamped; an auxiliary table (U-V) and wire drive mechanism. The main table moves along X and Y-axis and it is driven by the D.C servo motors. The travelling wire is continuously fed from wire feed spool and collected on take up spool which moves though the work piece and is supported under tension between a pair of wire guides located at the opposite sides of the work piece. The lower wire guide is stationary whereas the upper wire guide, supported by the U-V table, can be displaced transversely along U and V-axis with respect to lower wire guide. The upper wire guide can also be positioned vertically along Z-axis by moving the quill.

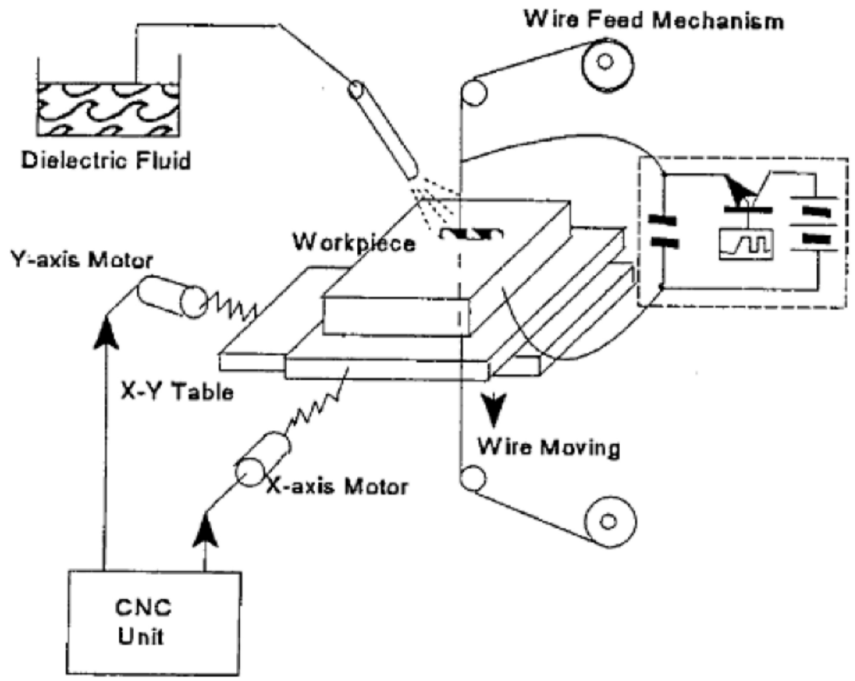

Figure 1.4 : Schematic of Wire Electric Discharge Machining Machine Tool

A series of electrical pulses generated by the pulse generator unit is applied between the work piece and the travelling wire electrode, to cause the electro erosion of the work piece material. As the process proceeds, the X-Y controller displaces the worktable carrying the work piece transversely along a predetermined path programmed in the controller. While the machining operation is continuous, the machining zone is continuously flushed with water passing through the nozzle on both sides of work piece. Since water is used as a dielectric medium, it is very important that water does not ionize. Therefore, in order to prevent the ionization of water, an ion exchange resin is used in the dielectric distribution system to maintain the conductivity of water. In order to produce taper machining, the wire electrode has to be tilted. This is achieved by displacing the upper wire guide (along U-V axis) with respect to the lower wire guide. The desired taper angle is achieved by simultaneous control of the movement of X-Y table and U-V table along their respective predetermined paths stored in the controller. The path information of X-Y table and U-V table is given to the controller in terms of linear and circular elements via NC program. Figure 1.4 exhibits the schematic diagram of the basic principle of WEDM process.

1.5 Problem Formulation

Parametric analysis has been done by conducting a set of experiments using air as the dielectric medium. Effect of the input parameters such as gap voltage, discharge current, pulse-on time, duty factor, inlet air pressure and spindle speed on material removal rate (MRR) and surface finish (Ra) has been studied. An empirical model for MRR and Ra has then been developed by conducting a designed experiment based on the Central Composite Design (CCD). The current work aims following

- Experimental investigation of EDM process parameters
- Parametric and Regression Analysis of Experimental Results
- ANN Model is developed for EDM parameter optimization
- Validation of ANN model and Parametric (regression) model with experimental results.

CHAPTER 2

LITERATURE REVIEW

2.1 Introduction

It is conventional wisdom in the EDM community that a liquid dielectric is essential for conducting EDM operation. The first reference to dry EDM can be found in a 1985 NASA Technical report [2]. It is briefly reported that argon and helium gas were used as dielectric medium to drill holes using tubular copper electrode. Further details are however not available. Later in 1991, Kunieda et. al. [3] showed that introducing oxygen gas into the discharge gap improves MRR in a water based dielectric medium. It was in 1997 that the feasibility of using air as the dielectric medium was first demonstrated by Kunieda et al. [4]. High velocity gas jet through a thin walled tubular electrode was used to serve the purpose of a dielectric. Further research in this field has brought out some of the essential features of the process. It is now known that some of the advantages of the dry EDM process are: low tool wear, lower discharge gap, lower residual stresses, smaller white layer and smaller heat affected zone [4-7].

Also, several studies have been made to improve the performance of the process [8-13]. However, the knowledge base in dry EDM is still limited to such an extent that an accurate prediction of process performance is not possible for a given set of input variables. The relevant literature and its significance in dry EDM research have been discussed below. The work by Kuniedaet. al. [3] not only demonstrated that EDM in gaseous medium is possible but also brought out some of the advantages of the process. Their work showed that high velocity gas flow through tool electrode reduces debris reattachment after a spark, thus considered to be effective in flushing. The debris reattachment is much lower for a thin walled tube and this increases the MRR. It was found that the probability of short circuits reduces when rotation or planetary motion is given to the tool electrode.

It was also shown that the tool wear ratio (TWR) is almost zero in dry EDM. MRR is shown to increase when oxygen gas is used and it is suggested that the heat generated by oxidation is responsible for the increased MRR. Dry EDM was applied to 3D machining using an NC tool path and precise machined shapes were obtained. It was also observed by them that the MRR increases when the concentration of oxygen in the dielectric gas mixture is increased. The effect of tool rotation on MRR, tool wear and surface finish has been experimentally studied in oil-die sinking EDM by Soni et al. [14]. Experiments were conducted with a rotating copper-tungsten tool electrode for oil die-sinking EDM of titanium work-piece. Designed experiments were conducted to compare rotary EDM with stationary tool EDM. It was found that rotation of the tool leads to a higher sparking efficiency and a better flushing of debris from the discharge gap consequently leading to a higher MRR. However, a poorer surface finish was obtained with a rotating tool. It was also observed that a statistically significant effect of tool rotation on tool wear did not exist. Kunieda et. al. [5] proposed that dry EDM is not only a thermal process but also a chemical process. With oxygen gas used as the dielectric medium, three distinct modes of material removal were observed depending on the discharge power density: normal mode, quasi-explosion mode and explosion mode. Thermally activated oxidation of work piece material becomes uncontrolled at very high discharge powers leading to uncontrolled arcing in the explosion mode. In the quasi-explosion mode there is no discharge delay time and the oxidation reaction is controllable since the reaction stops as soon as the power is switched off. The material removal rate during quasi-explosion mode was found to be as high as in a conventional milling process; however the tool wear was still low.

Also, an alternate ‘intake method’ of gas supply in the gap was proposed for improving the accuracy. Instead of supplying gas through the hollow tool electrode, gas was sucked into the tool electrode in the ‘intake method’. Yu et. al. [6] demonstrated the effectiveness of the dry EDM method in machining of cemented carbide. Dry EDM was used for groove milling and three-dimensional milling. Copper-tungsten tubes were used as tool electrodes and high velocity oxygen gas was used as the dielectric. Dry EDM performance was compared to oil die sinking EDM and oil EDM milling. It was found that dry EDM milling produces the smallest form deviation due to very low tool wear ratio. The machining speed in dry EDM is higher than for oil milling EDM but

lower than oil die-sinking EDM. However, it was argued that the total time required for making multiple electrodes in die-sinking EDM puts it at a disadvantage to dry EDM milling. Fewer tool electrodes are required in dry EDM due to lower tool wear. The total machining time for dry EDM may then be lower than die-sinking EDM. Kunieda et. al. [7] has used a piezoelectric actuator to improve the dry EDM characteristics by controlling the discharge gap distance. The work-piece was mounted on a piezoelectric element and the control signal to the element was provided by a feedback from the actual average gap voltage. The element had a high frequency response (natural frequency of 500MHz) and the control system was responsible for providing the displacement command signal to the piezoelectric element. Experiments were conducted with the piezo control. It was found that presence of the actuator leads to a reduction in the arcing probability and increases the MRR by improving the stability of the process. The arcing probability and MRR improvement were also predicted through simulation of the process. It was found that the simulation over-estimates the performance improvement. From simulations it was also found that conventional is stable enough even in the absence of the piezoelectric servo system. Based on experiments and simulation it was found that monotonous oscillations (such as a sine wave) of the piezo element were not as advantageous in improving process stability as the servo control system. Zhanbo et. al. [8] demonstrated the feasibility of 3D surface machining using dry EDM. The developed process was used for micromachining applications. Parametric analysis was done to observe the effect of gas pressure, depth of cut, pulse duration, pulse interval and rotational speed of tool electrode on MRR and tool wear ratio (TWR). It was found that optimum conditions exist for gas pressure, depth of cut and pulse duration for achieving maximum MRR and minimum TWR.

It is suggested that at high gas pressure debris removal is enhanced, however frequent short circuits were observed for very high pressure values. MRR is found to saturate to a constant value for tool rotational speeds above 500 RPM. At very low RPM values, frequent short circuits occur due to poor debris removal. The dry EDM process has been used for EDM milling and contouring on micro scales. Zhang et. al. [9] and Zhang et. al. [10] proposed an improvement over dry EDM by introducing ultrasonic vibrations to the work-piece. A mathematical model for MRR in terms of process parameters (open voltage, discharge current, pulse duration and pulse interval) was also

developed. It was experimentally found that MRR increases with decrease in tool wall thickness and increase in open voltage, pulse duration, discharge current and amplitude of ultrasonic vibration. It was also found that surface roughness increases with pulse duration. Surface roughness however does not show any clear dependence on amplitude of vibration or tool wall thickness. This work presented ultrasonic EDM in gas however it failed to compare the performance of dry UEDM with liquid-dielectric EDM processes. The dry EDM process has been used for precision wire EDM (WEDM) cutting by Kunieda et. al [11]. Lower reaction forces and electrostatic forces are produced during dry WEDM as compared to conventional WEDM with water. Dry WEDM was performed with brass wire in the atmosphere without any external dielectric supply to the discharge gap. WEDM experiments were performed with water as dielectric and in the dry conditions. Effects of current, wire winding speed and depth of cut on MRR, straightness, surface roughness, waviness and gap length were investigated. It was found that better straightness of cut and surface finish is obtained in dry WEDM and the gap length is narrower in dry WEDM.

In addition, no over-cut was observed in dry WEDM because of smaller distortion and vibration of the wire. However, it was found that the waviness and the MRR were poorer in dry WEDM due to frequent short circuiting. Improving the frequency response of the wire feed control has been suggested to reduce short circuiting. From the experiments it was also found that increasing the wire winding speed and decreasing the depth of cut could lead to an improvement in MRR and waviness. Kao et. al. [12] have further investigated the dry WEDM process for thin work pieces. Experiments were carried on with different work-piece materials and it was found that work-piece thickness, melting temperature and heat capacity had significant effect on machinability. Dry WEDM experiments were performed using a copper electrode wire in stationary air or with an assisting air jet. Experiments were performed to investigate the effects of duty factor, pulse-on time, air flow rate and work-piece thickness on MRR, groove width, debris deposition and the rate of spark, arc and short pulses. Analysis of the measured voltage and current was done to identify the spark, arc and short pulses. Lower values of MRR were obtained in dry WEDM, but the MRR could be slightly improved by the use of air flow. It was found that MRR reduces with an increase in the work-piece thickness and the work piece melting temperature. The MRR was found to be

related to the rate of spark, arc and short pulses. Very recently, Tao et. al. [13] have experimentally investigated the dry and near dry EDM process. A two phase gas-liquid mixture was used as the dielectric medium in near dry EDM. Commercially available rotary spindle with through-spindle flushing capability was used for implementing dry and near dry EDM. The effect of discharge current, pulse-duration, pulse interval, gap voltage and open circuit voltage was investigated at constant values of gas pressure and tool rpm by using a 2^{5-1} fractional factorial designed experiment. Separate set of input parameter values and tool-dielectric combinations were identified for finish and rough machining. It was found that copper tool and oxygen gas dielectric with a high current and low pulse off time were suitable for rough machining with a high MRR. Graphite tool and water nitrogen gas mixture was found to give a better surface finish. Low current, low pulse-on time and high pulse-off time was found to be suitable for finishing operations. Ra values, as low as 0.8 μm, have been reported in the near dry EDM finishing conditions.

In the past few decades, a few EDM modeling tools correlating the process variables and surface finish have been developed. Tsai and Wang [1] established several surface models based on various neural networks taking the effects of electrode polarity in to account. They subsequently developed a semi-empirical model, which dependent on the thermal, physical and electrical properties of the work piece and electrode together with pertinent process parameters. It was noted that the model produces a more reliable surface finish prediction for a given work under different process conditions [2]. Jeswani *et al.,* [3] studied the effects of work piece and electrode materials on SR and suggested an empirical model, which focused solely on pulse energy, whereas, Zhang *et al.,* [4] proposed an empirical model, built on both peak current and pulse duration, for the machining of ceramics. It was realized that the discharge current has a greater effect on the MRR while the pulse-on time has more influence on the SR and white layer. Lin *et al.,* [5] employed gray relational analysis for solving the complicated interrelationships between process parameters and the multiple performance measures of the EDM process. Marafona and Wykes [6] used the Taguchi method to improve the TWR by introducing high carbon content to the electrode prior to the normal sparking process. Lin *et al.,* [7] employed it with a set of fuzzy logic to optimize the process parameters taking the various performance measures in to

consideration. Tzeng and Chen [8] optimized the high speed EDM process by making use of dynamic signal to Noise ratio to classify the process variables in to input signal, control and noise factors generating a dynamic range of output responses. Kesheng Wang *et al.,* [9] discussed the development and application of hybrid artificial neural network and genetic algorithm methodology to modeling and optimization of electric discharge machining. But, they considered only the pulse on time and its effect on MRR. OguzhanYilmaz *et al.,* [10] used a user friendly fuzzy based system for the selection of electro discharge machining process parameters. Effect of other important parameters like current, voltage and machining time on TWR, SR, over cut and hardness is not considered. Even though efforts were made by some authors [11-16] to characterize the discharge machining of new materials like Ti6Al4V, 15CDV6 etc, modeling and optimization using hybrid technique was not attempted.

The EDM process has a very strong stochastic nature due to the complicated discharge mechanism [17] making it too difficult to optimize the sparking process. In several cases, S/N ratios together with the analysis of variance (ANOVA) techniques are used to measure the amount of deviation from the desired performance measures and identify the crucial process variables affecting the process responses. A vast majority of the research work have been concerned with the improvement made to the performance indices, such as MRR, TWR and SR. Hence, a constant drive towards appreciating the MRR, TWR and metallurgy of EDMEd surface will continue to grow with the intension of offering a more effective means of improving the performance measures. Furthermore, the traditional EDM will gradually evolve towards micro electro discharge machining (MEDM) by further manipulating the capability of computer numerical control (CNC) but the MRR will remain a prime concern in fulfilling the demand of machining part in a shorter lead-time.EDM has made a significant inroad in the medical, optical, dental and jewelry industries, and in automotive and aerospace R and D areas [18]. An attempt has been made by Yin Fong Tzeng et al. [19] to present a simple approach for optimizing high speed electric discharge machining. These applications demand stringent machining requirements, such as the machining of high strength temperature resistant (HSTR) materials, which generate strong research interests and prompt EDM machine manufacturers to improve the machining characteristics.

With regard to characterization of materials on EDM it is found that recently developed materials like Ti6Al4V, HE15, 15CDV6 and M250 are not explored till now. It is further proved that much work has not been done to create a model, which can predict the behavior of these materials when they are discharge machined. The scattered work done in the area of modeling does not include all-important parameters such as current, voltage and machining time. Hence, in light of the available literature it is aimed to address EDM on recently developed materials like Ti6Al4V, HE15, 15CDV6 and M250 considering different input variables for optimum solution with an aim to optimize MRR. Finding an optimal solution by creating a model of the process using neural network and then selecting the weights with the help of genetic algorithms is the main objective of present study.

CHAPTER 3

THEORETICAL BACKGROUND

3.1 EDM Discharge Phenomena

Phases of discharge

The discharge process during EDM can be separated into three main phases [15]. They are: preparation phase, discharge phase and interval phase. Details of each phase are discussed below.

Preparation phase

On switching on the power supply, electric field is set-up in the gap between the electrodes. The electric field reaches maximum value at the point where the gap between the electrodes is smallest. Spark location is determined by the gap distance and the gap conditions. In the presence of electrically conductive particles in the gap, thin particle bridges are formed. When the strength of the electric field exceeds the dielectric strength of the medium, electric breakdown of the medium takes place. Ionization of the particle bridges takes place and a plasma channel is formed in the gap between the electrodes. The steps in the phase are shown in Figure 2.1 (a).

Discharge phase

During the discharge phase (Figure 2.1 (b)), a high current flows through the plasma channel and produces high temperature on the electrode surfaces. This creates very high pressure inside the plasma channel creating a shock wave distribution within the dielectric medium. The plasma channel keeps continuously expanding and with it the temperature and current density within the channel decreases. Plasma channel diameter stabilizes when a thermal equilibrium is established between the heat generated and the heat lost to evaporation, electrodes and the dielectric. This enlarged channel is still under high pressure due to evaporation of the liquid dielectric and material from the electrodes. The evaporated material forms a gas bubble surrounding the plasma

channel. During this phase, high energy electrons strike the work piece and the positively charged ions strike the tool (for negative tool polarity). Due to low response time of electrons, smaller pulses show higher material removal from the anode whereas; longer pulses show higher material removal from the cathode.

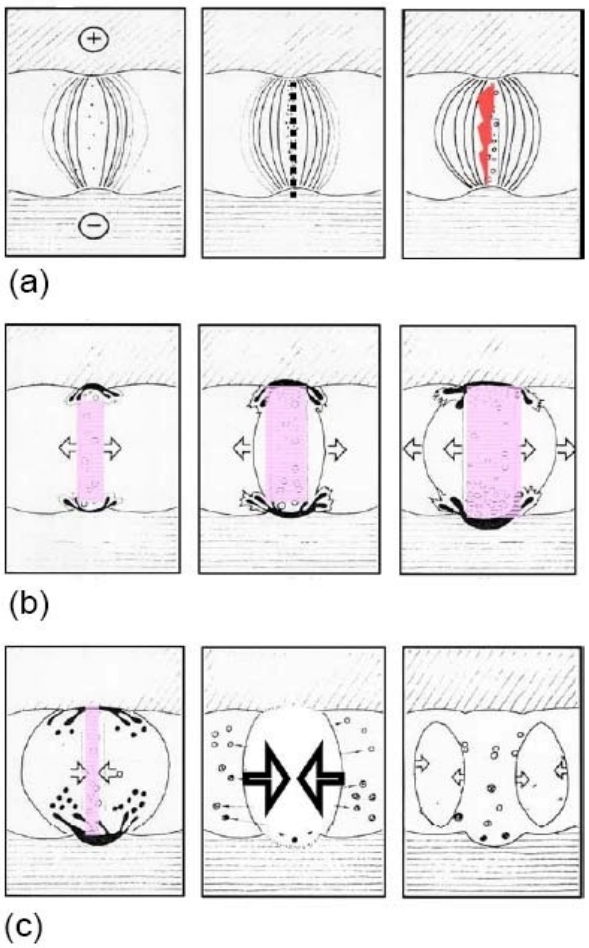

Figure 3.1: Phases of a discharge during EDM. (a) Preparation phase (b) Discharge phase (c) Interval phase

Internal Phase

The plasma channel de-ionizes when power to the electrodes is switched off. The gas bubble collapses and material is ejected out from the surface of the electrodes in the form of vapors and liquid globules. The evaporated electrode material solidifies quickly when it comes in contact

with the cold dielectric medium and forms solid debris particles which are flushed away from the discharge gap. Some of the particles stay in the gap and help in forming the particle bridges for the next discharge cycle. Power is switched on again for the next cycle after sufficient de-ionization of dielectric has occurred. The steps in the phase are shown in Figure 3.1 (c).

3.2 Effect Of Input Parameters

Based on the discharge phenomena discussed above, the effect of various input parameters on material removal rate (MRR) and surface roughness (Ra) is discussed below.

Discharge Current

The discharge current (I_d) is a measure of the power supplied to the discharge gap. A higher current leads to a higher pulse energy and formation of deeper discharge craters. This increases the material removal rate (MRR) and the surface roughness (Ra) value. Similar effect on MRR and Ra is produced when the gap voltage (V_g) is increased.

Pulse-on time

Machining takes place only during the pulse-on time (T_{on}). When the tool electrode is at negative potential, material removal from the anode (work piece) takes place by bombardment of high energy electrons ejected from the tool surface. At the same time positive ions move towards the cathode. When pulses with small on times are used, material removal by electron bombardment is predominant due to the higher response rate of the less massive electrons. However, when longer pulses are used, energy sharing by the positive ions is predominant and the material removal rate decreases. When the electrode polarities are reversed, longer pulses are found to produce higher MRR.

Pulse-off time

A non-zero pulse off time is a necessary requirement for EDM operation. Discharge between the electrodes leads to ionization of the spark gap. Before another spark can take place, the medium must de-ionize and regain its dielectric strength. This takes some finite time and power must be switched off during this time. Too low values of pulse-off time may lead to short-circuits and

arcing. A large value on the other hand increases the overall machining time since no machining can take place during the off-time. The surface roughness is found to depend strongly on the spark frequency. When high frequency sparks are used lower values of Ra are observed. It is so because the energy available in a given amount of time is shared by a larger number of sparks leading to shallower discharge craters.

Gas Pressure

Apart from the electrical parameters, pressure of the gaseous dielectric may have an effect on the process performance during dry EDM. Velocity of the gas jet (Figure 1.3) is directly proportional to the inlet gas pressure. A high velocity gas jet would lead to better flushing of debris from the discharge gap thus improving the MRR and Ra values. Forced flow of gas also helps in reducing the time required for recovery of dielectric strength of the medium since fresh and previously non-ionized medium is continuously supplied to the gap. This leads to higher process stability. Also, it is found that the dielectric strength of air is dependent on the pressure and increases with an increase in the pressure. This favors an increase in the MRR of the process.

Tool rotation

Tool electrode rotation is commonly used in small-hole EDM drilling operations. Tool rotation improves flushing and leads to a more uniform electrode wear. The effects of improved flushing are an increased MRR and lower Ra value. At the same time, process stability increases because tool rotation makes it easier to introduce fresh dielectric into discharge gap as the used up dielectric is thrown out due to the centrifugal force. Thus, even with low pulse off times and poor flushing conditions good machining performance is obtained.

3.3 Dielectric Medium in EDM

Functions of dielectric

Dielectric fluid plays an important role in the EDM process. Because of a high dielectric strength, the dielectric medium prevents premature discharge between the electrodes until a low discharge gap is established between them. Continuous dielectric flow in the discharge gap helps in carrying away the debris formed during the discharge and ensures a proper flushing. Also, dielectric medium cools the machining zone by carrying away excess heat from the tool electrode and the

work-piece.

Properties of dielectric

The most important properties of dielectric are its dielectric strength, viscosity, thermal conductivity and thermal capacity. Dielectric strength characterizes the fluid's ability to maintain high resistivity before spark discharge and the ability to recover rapidly after the discharge. High dielectric strength leads to a lower discharge gap which in turn leads to a low gap resistance. Hence, high discharge currents may flow leading to a higher material removal rate. Also, fluids with high dielectric strength need lower time for the recovery of dielectric strength. Thus, low pulse-off times are sufficient. This not only improves the MRR but also provides better cutting efficiency because of a reduced probability of arcing. Liquids with low viscosity generally provide better accuracies because of a better flow ability of the oil leading to improved flushing. Also, the sideward expansion of the discharge plasma channel is restricted by high viscosity fluids. This focuses the discharge energy over a small region and leads to a deeper crater which reduces the surface finish. [4]. Dielectric fluids with high thermal conductivity and thermal heat capacity can easily carry away excess heat from the discharge spot and lead to a lower thermal damage.

Types of dielectric

Selection of dielectric medium is an important consideration for EDM performance. Mineral oils are commonly used as the dielectric medium for die-sinking EDM operations. Mineral oils exhibiting high dielectric strength and a low viscosity are preferred because of their higher performance. For safety reasons oils with a high flash point are usually used. Kerosene is one such oil which is used commonly for EDM. Water based dielectrics are used almost extensively for wire EDM operations. Water has a high specific heat capacity which leads to a better cooling effect required for wire cut operations. To prevent chemical reactions, deionized water is used in such applications.

Table 3.1: Comparison of electrical, thermal and mechanical properties of mineral oil, deionized water and air

Properties	**Dielectric Strength**	**Dynamic Viscosity**	**Thermal Conductivity**	**Specific heat capacity**
Medium	(MV/m)	g/m-s	W/m-K	J/g-K
Kerosene	14-22	1.64	0.149	2.16
Deionized water	13	0.92	0.606	4.19
Air	3	0.019	0.026	1.04

In comparison to mineral oils and water, air has the lowest dielectric strength, viscosity, thermal conductivity and thermal capacity as shown in Table 2.1. A low viscosity air medium favors higher cutting accuracy and better surface finish. However, low dielectric constant suggests a lower MRR with air medium. Low thermal capacity and thermal conductivity suggests higher thermal damage of work piece. However, for a complete analysis of the thermal damage an opposing effect caused by the expansion of plasma channel due to low viscosity must also be accounted. Thus, overall it seems that using air as dielectric may be a better alternative for improving some of the process performance such as surface finish and accuracy at the expense of the MRR.

3.4 Mathematical Models

Model for MRR

Material removal rate (MRR) refers to the amount of material removed from the work piece per unit time. It can be estimated in terms of the electrical parameters as: the amount of material removed per spark multiplied by the number of sparks per unit time. The amount of material removed per spark is proportional to the volume of the discharge crater (V_c). The volume of discharge crater depends on the spark energy (E_s). This gives:

$$V_c = K_1 E_s \tag{3.1}$$

Where K1 is proportionality constant

The spark energy is given by:

$$E = V_g I_d T_{on} \quad (3.2)$$

Assuming that one spark occurs over each pulse-on time, the spark frequency (f) is given by:

$$f = \frac{1}{T_{on} + T_{off}} \quad (3.3)$$

Since,

$$MRR = fVc$$

$$MRR = k \frac{V_g I_d T_{on}}{T_{on} + T_{off}} \quad (3.4)$$

kis the proportionality constant.

Effect of the non-electrical parameters such as inlet gas pressure (P) and spindle rpm (N) is included in the proportionality constant 'k'.

It is interesting to note at this stage that Eq. 3.3 may not give an accurate estimate of spark frequency for a rotating tool. For stationery tool EDM, spark can occur continuously throughout the spark-on time and the assumption that only one spark occurs over a pulse-on time can be justified. However, for a rotating tool the spark may be interrupted due to the movement of the tool during the pulse-on time. Under such circumstances, several short sparks may occur over a single spark-on time, at locations where the instantaneous spark gap is lowest. Thus the spark frequency may be much higher than given by Equation 3.3. Such an anomaly would be more pronounced at higher pulse-on times and Equation 3.3 is expected to be in reasonable agreement with experiments at low pulse-on time values.

Model for surface roughness

Roughness of the surface obtained after performing dry EDM is quantified by the center line average roughness value (Ra). The functional dependence of Ra on the parameters can be estimated by performing a dimensional analysis based on the Buckingham π theorem. With six parameters and three dimensions: mass (M), length (L) and time (T), three dimensionless π

parameters would be required. The parameters and their corresponding dimensions are shown in Table 2.2. The basis chosen for dimensional analysis is: (W, T_{on}, P).

Table 3.2: Parameters and their corresponding dimensions for dimensional analysis of surface roughness value

Parameter	Symbol	Unit	Dimension
Surface roughness	Ra	Mm	L
Electric power	W(=V_g*I_d)	watt	ML^2T^{-3}
Pulse-on time	T_{on}	Ms	T
Pulse-off time	T_{off}	Ms	T
Gas pressure	P	kgf/cm^2	$ML^{-1}T^{-2}$
Spindle rpm	N	rpm	T^{-1}

The π parameters can be represented as:

basis :(W, T_{on}, P)

$$\pi_1 = W^{\alpha 1} T_{on}^{\beta 1} P^{\gamma 1} Ra$$

$$\pi_2 = W^{\alpha 2} T_{on}^{\beta 2} P^{\gamma 2} T_{off}$$

$$\pi_3 = W^{\alpha 3} T_{on}^{\beta 3} P^{\gamma 3} N \qquad (3.5)$$

Substituting the dimensions for each parameter and equating dimensions on both sides of the equations gives:

$$(\alpha_1 \beta_1 \gamma_1) = \frac{1}{3}(-1.-1,1)$$
$$(\alpha_2 \beta_2 \gamma_2) = (0,-1,0)$$
$$(\alpha_3 \beta_3 \gamma_3) = (0,1,0)$$

Thus, the dimensionless π parameters are:

$$\pi_1 = \left(\frac{P}{V_g I_d T_{on}}\right)^{1/3}$$

$$\pi_2 = \left(\frac{T_{off}}{T_{on}}\right)$$

$$\pi_3 = T_{on}\, N \tag{3.6}$$

Representing π1 as a function of π2 and π3 and substituting for the π parameters gives:

$$\pi_1 = f(\pi_2, \pi_3)$$

$$Ra = \left(\frac{V_g I_d T_{on}}{P}\right)^{\frac{1}{3}} f\left(\frac{T_{off}}{T_{on}}, T_{on}\, N\right) \tag{3.7}$$

Volume of the discharge crater is proportional to the spark energy and the depth of crater scales as 1/3rd of the crater volume. Hence, surface roughness is expected to be proportional to cube root of current and voltage. Dimensional analysis yields a similar dependence of Ra on V_g and I_d. Eq. (3.7) also shows that the Ra value decreases with an increase in the gas inlet pressure (P). Additional information (such as from experiments) is required to obtain the exact form of the function 'f'.

3.5 Design of Experiments (DOE)

DOE principles

Design of Experiments (DOE) refers to planning, designing and analyzing an experiment so that valid and objective conclusions can be drawn effectively and efficiently [16]. In performing a designed experiment, changes are made to the input variables and the corresponding changes in the output variables are observed. The input variables are called factors and the output variables are called response. Factors may be either qualitative or quantitative. Qualitative factors are discrete in nature (such as type of material, color of sample). Each factor can take several values during the experiment. Each such value of the factor is called a level. A trial or run is a certain combination of factor levels whose effect on the output is of interest. It is convenient to represent the high level value of a factor as +1 and the low level value as -1, and transforming all the factors into the same [-1 1] coded range. It is essential to incorporate statistical data analysis methods in the experimental design in order to draw statistically sound conclusions from the experiment.

Some of the advantages of DOE over One-Variable-At-a-Time approach (OVAT) are that a DOE approach enables to separate the important factors from the unimportant ones by comparing the factor effects. Also, interaction effects among different factors can be studied through designed experiments.

Response Surface Methodology

Response Surface Methodology (RSM) is a collection of statistical and mathematical techniques useful for developing, improving and optimizing processes [17]. RSM is useful for the modeling and analysis of experiments in which a response of interest is influenced by several variables and the objective is to optimize this response. Consider a process where the response variable (output) y depends on the controllable (input) variables x_1, x_2, …,x_k. The relationship is:

$$y = f(x_1, x_2, \ldots\ldots x_k) \qquad (3.8)$$

The true form of the response variable y is seldom known for a process. In RSM, the true relationship between y and the independent variables is generally approximated by the lower-order polynomial models such as:

$$y = \beta_0 + \beta_1 x_1 + \cdots + \beta_k x_k + \varepsilon$$

$$y = \beta_0 + \sum_{i=1}^{k} \beta_i x_i + \sum_{i=1}^{k} \beta_{ii} x_i^2 + \sum_{i<j} \beta_{ij} x_i x_j + \varepsilon \qquad (3.9)$$

Where ε represents the statistical error term

Here, the βs are the unknown parameters. These parameters are estimated by first collecting data on the system and then performing statistical model building by using regression analysis. Response surface designs are special types of experimental designs which are commonly used for the data collection phase. Polynomial models are generally linear functions of the unknown βs. Hence linear regression is used for the model building phase. A linear regression model may be written in matrix notation as:

$$Y = X\beta + \varepsilon$$

Where

$$y = (y_1, y_2, \ldots \ y_n)^T, \quad X = \begin{pmatrix} 1 & x_{11} & \ldots x_{1k} \\ \vdots & \vdots & \ddots \ \vdots \\ 1 & x_{n1} & \ldots x_{nk} \end{pmatrix}$$

$$\beta = (\beta_1, \beta_2, \ldots \ \beta_n)^T, \quad \varepsilon = (\varepsilon_1, \varepsilon_2, \ldots \ \varepsilon_n)^T$$

(3.10)

In general, y is an (n x 1) vector of the responses, X is an (n x p) matrix of the levels of the independent variables, β is a (p x 1) vector of the regression coefficients and ε is an (n x 1) vector of random errors, with p=k+1.

The least square estimate of the β parameters is:

$$b = (X'X)^{-1}X'y \qquad (3.11)$$

The fitted regression model is:

$$y = X b \qquad (3.12)$$

Central Composite Design

The central composite design (CCD) is one of the most popular classes of designs used for a second-order model. CCD designs comprise a set of two-level factorial points, axial points and center runs. The factorial points contribute to the estimation of linear terms and two-factor interactions. Factorial points are the only points which contribute to estimation of the interaction terms. The axial points contribute to the estimation of quadratic terms. In the absence of axial points, only the sum of the quadratic terms can be estimated. The center runs provide an internal estimate of pure error and contribute towards the estimation of quadratic terms. The number of factorial runs depends on the type of factorial design used and the number of factors. A minimum design resolution of V is required for the factorial fraction. For a full factorial, there are 2^k factorial points. The number of axial points is 2k and the number of center runs (n_c) depends on the number of factors.

For up to four factors, three to five center runs are sufficient. Higher number of center runs is preferable if there are more than four factors. The axial points lie at a distance of ± α from the center point (zero level for all factors). The value of α generally varies from 1 to √k. In the coded space, axial points are obtained by taking ± α level for one factor and the zero level for all other factors. Thus, there are 2k axial points, two points (one +α and one -α) for each factor. Each factor is varied over five levels: ± α (axial points), ± 1 (factorial points) and the center point.

3.6 Artificial Neural Network Model

An artificial neural network is an information-processing system that has certain performance characteristics in common with biological neural networks. Artificial neural networks have been developed as generalizations of mathematical models of human cognition or neural biology, based on the assumptions that:

1. Information processing occurs at many simple elements called neurons.
2. Signals are passed between neurons over connection links.
3. Each connection link has an associated weight, which, in a typical neural net, multiplies the signal transmitted.
4. Each neuron applies an activation function (usually nonlinear) to its net input (sum of weighted input signals) to determine its output signal.

In the past decades, numerous studies have been reported on the development of neural networks based on different architectures. Basically, one can characterize neural networks by its important features, such as the architecture, the activation functions, and the learning algorithms. Each category of the neural networks would have its own input output characteristics, and therefore it can only be applied for modeling some specific processes. In this work, ANN is employed for modeling and determination of optimal parameters for the EDM process

Architecture

Neural networks are in general categorized by their architecture. The number of hidden layers is critical for the convergence rate at the stage of training the network parameters. Empirically

speaking, one hiddenlayer6888should be sufficient in the multi-layered networks because the number of neurons is typically assumed to be dominant in the networks. In other words, the number of neurons must be determined by an optimization method. In this work, a multi-layer back-propagation network is adopted to model the EDM process. To be in particular, a four layer BP network with*6,14,18,2*neurons in each of the respective layers. This particular configuration gives the output values, which are nearer to the target set values with very little error. MATLAB software, which is a high-performance language for technical computing, is used for modeling and developing of neural network.

Activation Functions

The connections among the neurons are made by signal links designated by corresponding weightings. Each individual neuron is represented by an internal state, namely the activation, which is functionally dependent of the inputs. In general, the Sigmoid functions (S-shaped curves), such as logistic functions and hyperbolic tangent functions are adopted for representing the activation. In the networks, a neuron sends its activation to the other neurons for information exchange via signal links. In this work, two different functions for activation have been employed. They are *Linear transfer function* and *Tan-sigmoid transfer function*, in which the former is used for the output layer and the latter is used for the all hidden layers.

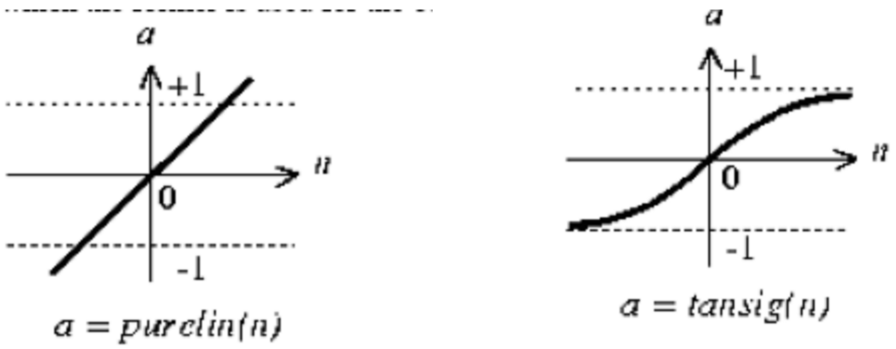

Figure 3.3: **a)** Linear transfer function, **b)** Tan-sigmoid transfer function

Algorithm

There are many variations of the back-propagation algorithm. The simplest implementation of back-propagation learning updates the network weights and biases in the direction in which the performance function decreases most rapidly - the negative of the gradient. One iteration of this algorithm can be written as $X_{k+1} = X_k - \alpha_k g_k$ where X_{k+1} is a vector of current weights and biases, X_k is the current gradient, and g_k is the learning rate. There are two different ways in which this algorithm can be implemented: incremental mode and batch mode. In the incremental mode, the gradient is computed and the weights are updated after each input is applied to the network. In the batch mode all of the inputs are applied to the network before the weights are updated.

Training

There are two back-propagation training algorithms: gradient descent, and gradient descent with momentum. These two methods are often too slow for practical problems. There are several high performance algorithms that can converge from ten to one hundred times faster than the algorithms mentioned above. All of the faster algorithms operate in the batch mode. These faster algorithms fall into two main categories. The first category uses heuristic techniques, which were developed from an analysis of the performance of the standard steepest descent algorithm. One heuristic modification is the momentum technique. There are two more heuristic techniques: variable learning rate back-propagation and resilient back-propagation.

CHAPTER 4

EXPERIMENTAL SET-UP AND PROCEDURE

4.1 Experimental Set-Up of EDM Machine

All the experiments have been conducted on a Z numerically controlled (NC) oil die-sinking EDM Machine, (R50 #ZNC). The EDM Machine is of Elektra, Electronica Machine Tools India make. In this machine, the Z axis is servo controlled and can be programmed to follow an NC code which is fed through the control panel. The servo control feedback is based on the gap voltage between the tool and the work piece electrodes. As machining takes place, the tool is fed into the work piece to maintain a constant gap voltage, and this determines the gap distance. The gap distance cannot be independently controlled on this machine. The X and Y axes are manually controlled. All three axes have an accuracy of 5µm. The machining time is displayed online during machining and is updated after every minute. Through an NC code, machining can be programmed to occur up to a fixed depth of cut. Alternately, sparks can be stopped manually after the desired time interval of machining has elapsed. The power supply system produces a DC pulsed power in the frequency range of 0.07 – 300 kHz. The pulse can be represented as shown in Figure 3.1. The pulse has been idealized by considering the pulse delay time as negligibly small. The pulse can be defined in terms of the gap voltage (V_g), discharge current (I_d), pulse-on time (T_{on}) and pulse-off time (T_{off}). An additional parameter, duty factor(d) can be represented in terms of the pulse on and off times as:

$$d = \frac{T_{on}}{T_{on} + T_{off}} \qquad (4.1)$$

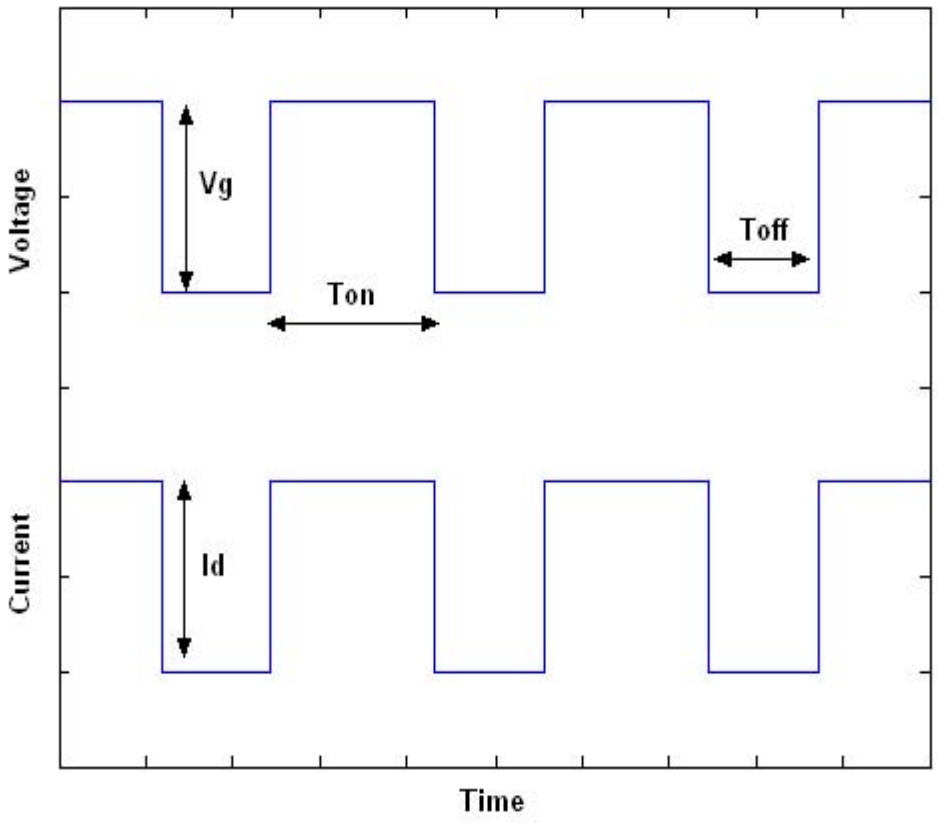

Figure 4.1: Graph of time vs. current & voltage

The control panel allows independent control of the gap voltage, discharge current, pulse on time and the duty factor. Corresponding to each Ton value, duty factor can be set to values between 8% and 96% in steps of 8%, subject to the maximum and minimum frequency limitations of the power supply. The duty factor is set by changing the duty factor position (D) on the control panel. Where:

$d = DX$ 8% (4.2)

During machining actual (time-average) values of discharge current and gap voltage can be read on the corresponding analog meters on the control panel. During machining arcing is sensed internally by the control system through an analysis of the current pulse. Power is switched off during a pulse if arcing is sensed. Anti-arc sensitivity determines the average percentage of arcing pulses for which power is switched off. If the anti-arc sensitivity is set to a low value then power

is switched off for a higher fraction of arcing pulses. The range and least count of various electrical parameters available on the machine are shown in Table 4.1.

Table 4.1: Range of values available on the ZNC EDM machine on which experiments have been conducted

Parameter	Range	In steps of
Gap Voltage	20 – 100 V	1 V
Discharge Current	1 – 50 A	1 A
Pulse on time	1 – 2000 μs	Available values: 1,2,5,10,20,30,50,75,100,150,200, 300,500,750,1000,2000 μs
Duty factor position	1-12	1 (each step corresponding to 8%)
Anti-Arc Sensitivity	1-10	1 (each step corresponding to 10%)

Dry EDM Unit Attachment

To enable performing the dry EDM process on existing EDM machines (which were originally designed for liquid dielectric only), a dry EDM unit attachment has been designed and developed. The dry EDM unit along with the ZNC EDM machine on which it is mounted is shown in Figure 3.2. The unit has been designed to fulfill the basic requirements of dry EDM: rotating tool and high velocity gas flow through tubular tool. Additionally, the entire arrangement is in the form of an independent unit which can be attached to existing EDM machines to perform dry EDM without any modifications in the existing machines. The dry EDM unit comprises a hollow spindle shaft supported on the flange of a cylindrical support through a pair of bearings. The shaft can rotate relative to the support cylinder. An O-ring sealing is provided at one of end of the shaft and a tool holder is mounted at the other end for holding tubular tools. The motor for spindle rotation is mounted on the support cylinder and power is transmitted from the motor through a belt-pulley system. Channel for high pressure gas flow is made in the support cylinder. A tube

transfers this gas from the support cylinder channel into the shaft-bore through the O-ring seal. The tubular tool mounted at the shaft end receives this high pressure gas while rotating relative to the support cylinder. Various parts of the attachment are shown in Figure 4.2. The dry EDM spindle can be functionally divided into five units. The functional units are:

- ✓ Main Support Structure
- ✓ Spindle Shaft
- ✓ Gas Inlet Unit
- ✓ Drive Unit
- ✓ Tool Holding Unit

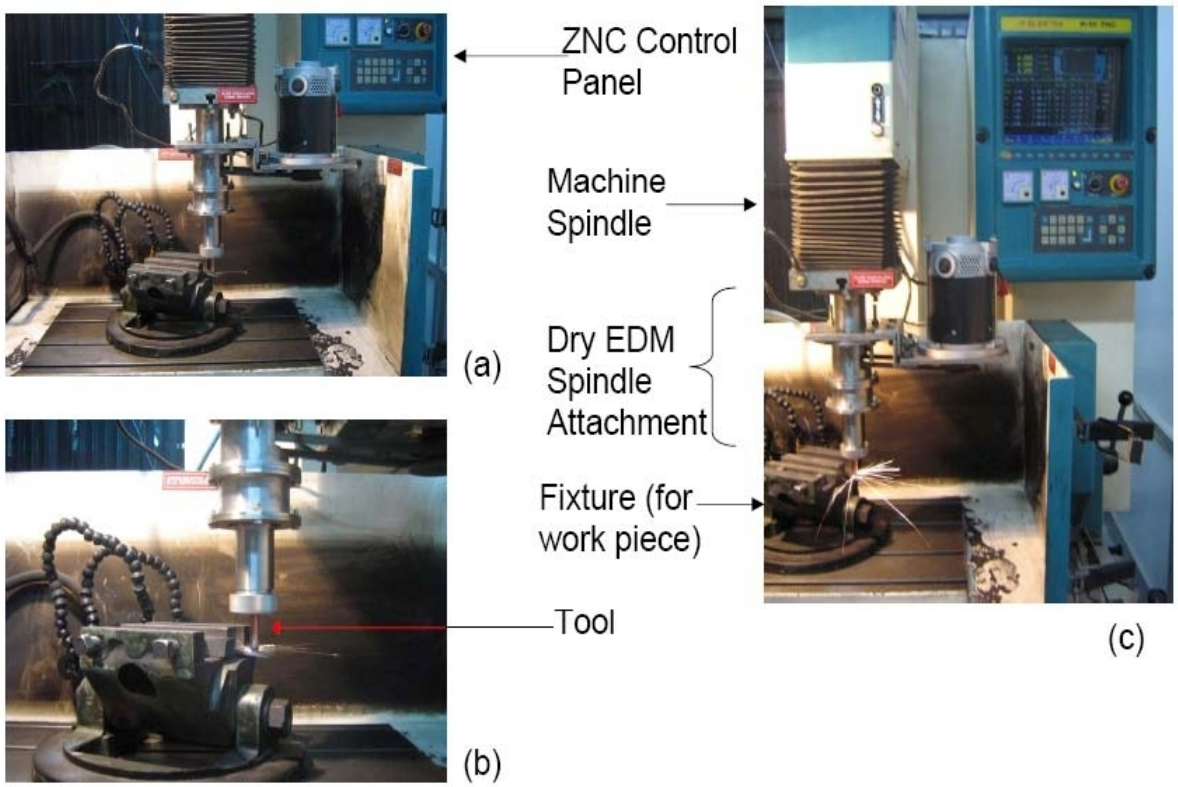

Figure 4.2: Dry EDM Unit Attachment

Main support structure

The main support structure consists of a cylindrical frame which can be attached to the machine spindle through bolts. The main body of the dry EDM spindle is attached separately to this

cylindrical structure. The main body consists of the spindle shaft which is supported axially through a pair of deep groove ball bearings. The shaft has a passage for gas through it.

Spindle shaft

The spindle shaft is in the form of a hollow cylinder. The shaft is rotated relative to the main support cylinder frame while high velocity gas is passed through it. Tubular tool electrode is mounted at the lower end of the shaft.

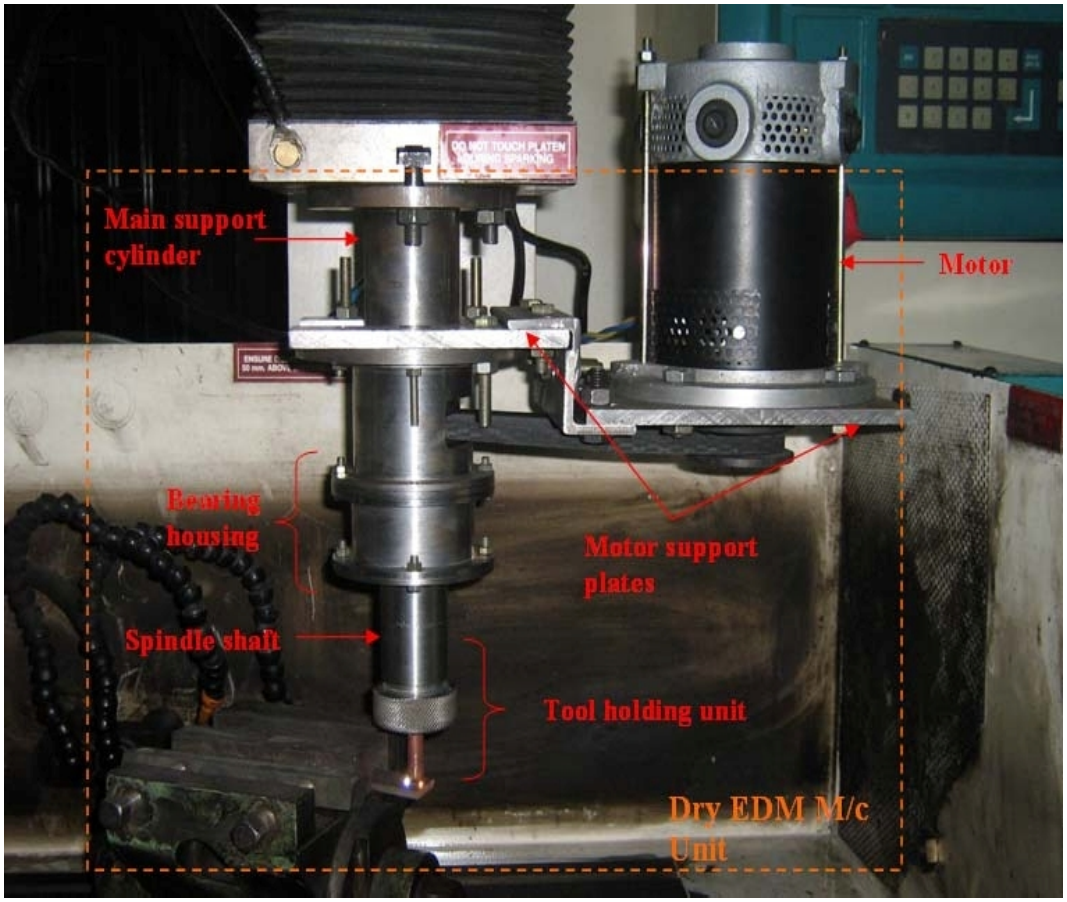

Figure 4.3: Dry EDM unit

Gas inlet unit

The gas inlet unit ensures that there is a path for continuous supply of high pressure gas through

the shaft during rotation. Gas inlet into the system is through a channel made in the main support cylinder. At the end of this channel a gas inlet tube is fitted to the cylinder. The gas inlet tube fits into the end of the shaft through the O-ring seal. The O-ring groove is designed for rotating shaft dynamic sealing [21]. This ensures a leak-free gas inlet into the rotating shaft.

Drive unit

Rotation to the shaft is provided by an electric motor. A 200W (at 1800 rpm) DC motor has been used to allow for continuous speed control from 300 rpm to 2250 rpm. Since the spindle moves along the vertical direction relative to the ground frame (during machining) due to the feed motion, the motor has to be supported on the spindle itself. The motor is side mounted on a platform which is joined to the main support structure, effectively forming a cantilever support frame for the motor. Power is transmitted from the motor to the spindle through a belt-pulley arrangement.

Tool holding unit

Tubular electrodes are used as the tool for dry EDM. The tool electrode is held in a collet chuck. For a leak free entry of gas from the spindle into the tool, an adapter is used which fits at the end of the shaft passage. One end of the adapter opens to the passage in the shaft and the other end has a tapered hole. The tool electrode sits on this tapered end.

Spindle Rotation and High Pressure Air Source

Spindle shaft is rotated by a DC motor which is mounted on the spindle itself. Continuous speed control in the range 300-2250 rpm is possible on the motor through a thyristor based control system. A rheostat control is provided on the motor control unit which can be used to increase or decrease the motor speed by changing the input voltage to the motor. Before starting with the experiments, the control unit is calibrated and the motor speeds corresponding to various rheostat positions are marked against it. During calibration, a mechanical tachometer (of least count 10 rpm) has been used to measure the motor RPM corresponding to a particular position of the rheostat. High pressure air is obtained from an ELGI make screw air compressor (E11-7.5) which has a built-in air drier. The compressor has a rated pressure of 7 kgf/cm^2 and a capacity of 1.81 m^3/min. At the inlet to the EDM machine a maximum gauge pressure of 2.5 kgf/cm^2 is obtained.

At the inlet, an air regulator with a regulation range of 0-10 bars has been used. A Bourdon tube pressure gauge with a least count of 0.1 kgf/cm^2 is used to monitor the inlet pressure to the dry EDM unit.

Work-piece and Tool

Experiments are conducted on EN32 mild steel (density 7.8 g/cm^3) work piece using a copper (density 8.9 g/cm^3) tool. The work piece is in the form of a thin strip of dimensions 75 mm x 20 mm x 5 mm. Small sized work pieces are used for ease of weight measurement on the balance. Tool electrode is in the form of a tube such that high velocity gas flows through it. The tool design is discussed in detail in the following sections.

Initial Tool Design: Single hole tube

During the exploratory experimental stage, experiments were first conducted using a thin walled tubular electrode with a centrally located single hole. It is found that use of such a tool leads to a central core formation during machining. The tube is shown in figure 4.4. Machining takes place only along the tube walls and no material is removed from the work-piece regions corresponding to the tube-central hole.

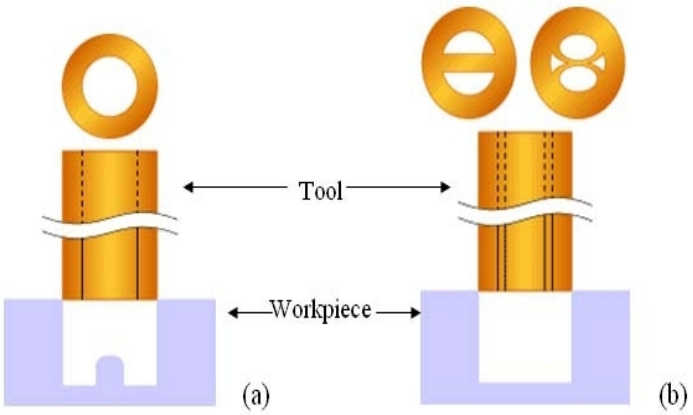

Figure 4.4: Central core formation

For a through hole machining, formation of the central core during machining does not pose any serious problem because eventually the central core falls off when the hole-drilling is complete

(similar to material removed during the trepanning operation). However, in such a case it is not possible to get an accurate MRR value for the process by using the weight measurement MRR calculation method used here. The material removed as the central core also adds to the MRR, but this material removal is not purely by the dry EDM process. Thus, a parametric study done for dry EDM process would not be accurate due to this "trepanning type material removal" contribution. When a blind hole is made using a single-hole tube, the central core remains on the work-piece. Due to its presence it is not possible to take surface roughness measurements on the bottom surface of the hole. To take measurements of the bottom surface of the hole it is important to eliminate the central core.

Insert-type multi-hole tool

In order to prevent the formation of a central core, a tube with non-central holes is used. Due to tube rotation the entire surface is exposed to sparks and no central core is formed. Due to the difficulty in manufacturing such tubes with high aspect ratio drilled holes, an insert type tool can be used, where a major portion of the tool (tool shank) consists of a tube with a large central hole and at the end of this tube, a cylindrical insert with non-central axial holes is fitted. The insert type tool is shown in figure 4.5.

There are two major problems with the insert type tools. First, if the axes of the outer cylindrical surface and the central hole in the main tube do not coincide (i.e. if the central hole is eccentric), then the insert would rotate eccentrically. Secondly, the gas-sealing at the insert-main tube junction poses a problem. It is not easy to ensure sealing at the junction without going for elaborate arrangement such as screw-threading or a proper press fit.

Single tube, multi-hole tool

Similar to the insert type tool, a single tube tool with non-central holes can be manufactured easily if the length of the non-central holes is small. Small non-central holes are drilled in a solid cylinder from one end. These holes open into a larger central hole which is drilled into the cylinder from the other end. The tool is shown in figure 4.5. This tool design has been selected for conducting the experiments. The top portion of the tool is made to the size of the holding collet. The outer diameter of the lower portion is determined by the diameter of the hole to be drilled.

The major problem with a single tube electrode is the large amount of material and time required for manufacturing the electrodes. It is observed that material is deposited on the tool during machining. Ideally each EDM operation should be carried on with a new tool electrode to take care of this effect. With the single tube design, a large number of electrodes would be required. Making such a tool requires more time and material than an insert type tool. To minimize the effect of debris which gets attached on the tool after machining, the tool face and sides are cleaned using emery cloth before starting a new experiment. This removes the deposited layer from the surface of the tool.

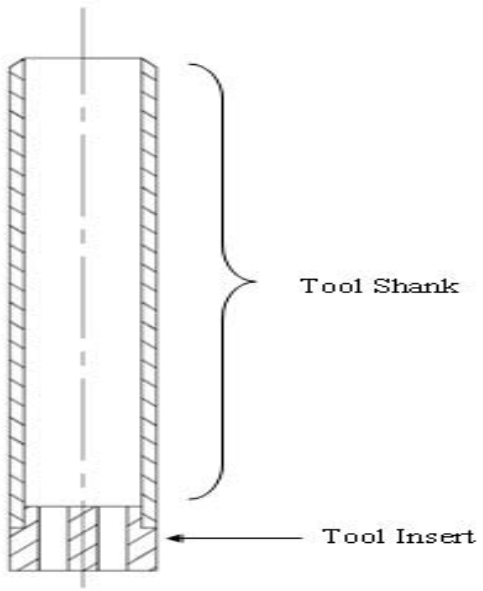

Figure 4.5: Single tube multi-hole tool

4.2 Experimental Procedure

Conducting Experiments: Standardization

Several controllable parameters such as the gap voltage discharge current, pulse-on time, duty factor position, air inlet pressure and spindle speed have been considered for analysis during the project. However, many other parameters which *may* have an effect on the output have not been studied. Some of these may be beyond our control (such as environmental conditions: room

temperature and humidity). However it may be possible to control some of them (such as Z motor sensitivity and anti-arc sensitivity). During the experiments it is essential to keep such parameters at some preset values so that data obtained from different runs are comparable. To ensure this, the following minimum standard has been maintained throughout all the experiments. Wherever necessary (and possible), extra precaution has been taken. The protocol is explained below:

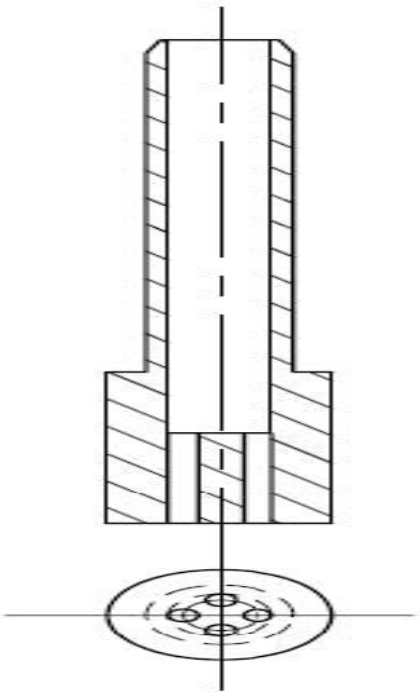

Figure 4.6: Multi-hole tool collet

For setting inlet gas pressure value

- ✓ The tool is first fixed in the spindle and the work piece is fixed in the fixture. The machine zero is then set and values of all electrical parameters are fed to the control panel.
- ✓ Motor for spindle rotation is started and the RPM value is approximately set to the desired value (using the calibration markings on the motor speed controller).
- ✓ The inter-electrode gap is set to 2 mm. It was observed that the pressure value (value indicated on pressure gauge) changed on changing the inter-electrode gap. The pressure value becomes more or less constant when the gap is more than 2 mm.

- ✓ Gas inlet valve is then switched on and the desired gas pressure is set using the regulator.

For making/finding zero gap tool position

- ✓ First the tool and work-piece are set.
- ✓ The tool is the brought near the work-piece surface and motor sensitivity value of '2' is selected. Motor sensitivity value determines the speed of the servo controlled Z-axis motor during the feed motion of the spindle. The speed of Z-axis motor is inversely proportional to the motor sensitivity value. Thus for a value of '1', the speed is low and for a value of '10' the speed is high. During sparking if the motor speed is too high it leads to instability due to frequent arcing. Hence the sensitivity value is set to as low as possible. However, it was observed that sometimes the servo motor was unable to produce enough starting torque at '1' setting and the spindle did not move along the Z axis. Hence the next higher value (setting '2') was chosen. The motor speed along Z axis is 40 mm/min at this setting.
- ✓ The 'APOS' operation was then selected on the machine control panel to set the machine zero.

For starting machining operation

- ✓ First the tool and work piece are set
- ✓ Machining zero (zero inter-electrode gap position) is then set
- ✓ Gas inlet pressure value is then set
- ✓ Spindle rpm is then verified by using a tachometer
- ✓ The tool-work piece gap is then to a preset value (=250 μm) and Z-motor sensitivity value of '2' is selected. It is important to standardize the initial gap value since MRR may depend on it. It is found that typically the spark gap in dry EDM is less than 100 μm. If the starting gap is set to a very high value, the machine takes a long time before the tool-work piece gap reduces to spark gap value and machining starts. On the other hand, a very small value may lead to arcing or short circuit. Hence the starting gap is set to an intermediate value of 250 μm.
- ✓ Finally, the 'SPARK' operation is selected on the control panel to start machining.

4.3 MRR and TWR Calculation

Material removal rate is calculated by measuring the loss in weight of the work piece after machining. The initial and final weights of the work piece are measured on Afcoset electronic balance (FX-400) having a resolution of 0.001 g. The weight material removal rate (MRRg) is then converted into volumetric material removal rate (MRRv) by knowing the density of the work piece material. An alternate method of MRR calculation is by measuring the depth of cut and then multiplying it with the area of cross-section of the cut. However, such a method may lead to faulty values if a constant area of cross-section is assumed since it is expected that the drilled section would be tapered. On the other hand, the weight loss method of MRR calculation gives the actual material removed during machining. Hence this method has been used for calculating the MRR. The weight loss method is also used for obtaining the tool wear rate. The tool is weighed before and after machining on the same balance as that used for the work piece. The weight TWR is converted into the volumetric TWR by knowing the density of tool material.

Surface Roughness measurement

Blind holes have been made by EDM during the experiments and the surface roughness of the end surface of the holes has been measured. The center line average (CLA) surface roughness parameter, Ra has been used to quantify the surface roughness of the machined surface. Ra (JIS 2001 standard) has been measured using a contact type stylus based surface roughness tester, MitutoyoSurftest SJ-301. Gaussian digital filter has been used for surface profile analysis using the instrument. The cut-off length is 0.8 mm and the evaluation length is 4 mm. Ra is measured along three different lines on the surface and the average value is considered for further analysis.

CHAPTER 5

RESULTS AND DISCUSSION

5.1 Exploratory Experiments

Exploratory dry EDM experiments were conducted by drilling blind holes in mild steel work-piece using a rotary cylindrical copper tube with multiple non-central holes for air flow. Results obtained from the experiments are discussed in the subsequent sections.

Depth of cut and machining time

For a particular set of input parameters, machining was done and the position of the tool face was recorded at regular time intervals. The variation of depth of cut with machining time is shown in Figure 5.1. From the figure it can be seen that the depth of cut increases linearly with time when sufficient cutting has taken place. However, for the first few minutes of machining, the depth of cut depends on the second power of the machining time. Based on the information derived from this figure it was concluded that experiments must be conducted for at least 8-10 minutes before stable cutting conditions can be achieved. It can also be seen from the 2nd order polynomial fitting function that the depth of cut corresponding to t=0 is negative. This negative value of depth of cut denotes the electrode gap distance at the start of machining.

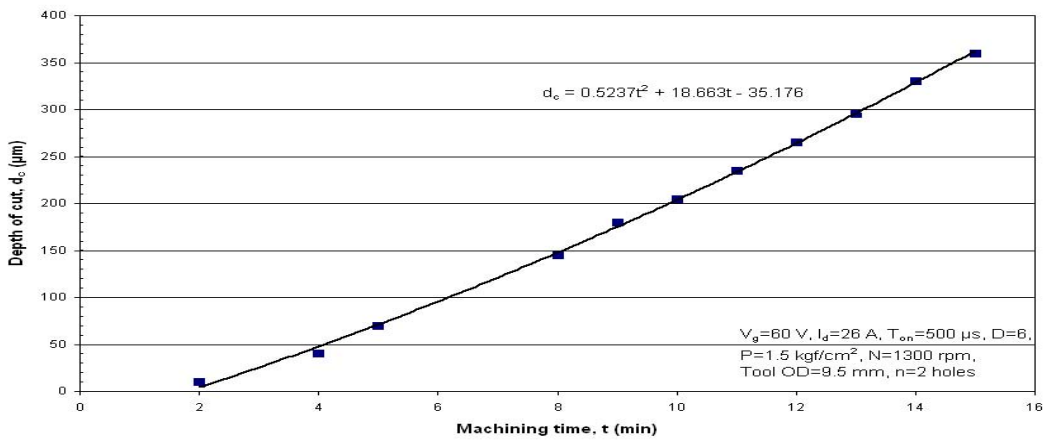

Figure 5.1: Variation of depth of cut with machining time

The effect of machining time on MRR and Ra is shown in Figure 5.2. Three experiments were conducted corresponding to each machining time and the average values of MRR and Ra are shown in the figure. It can be seen that MRR increases with an increase in the machining time. This effect can be attributed to the side-cutting taking place along the cylindrical face of the tool. As machining progresses, material is not only removed from the bottom surface of the hole in the work-piece but also from the sides of the hole. As machining takes place, more of the tool penetrates into the hole being machined in the work-piece and the length over which side-cutting takes place increases. This increases the MRR with machining time. Additionally, with reference to Figure 5.2, stable machining conditions are not established during the first few minutes of machining and the depth of cut increases quadratically with time. This explains the steep rise in MRR when machining time increases from 5 minutes to 10 minutes. For machining times greater than 10 minutes, the increase in MRR is less steep. Effect of machining time on Ra values is not as prominent since side cutting does not significantly affect the surface finish of the bottom surface of the hole.

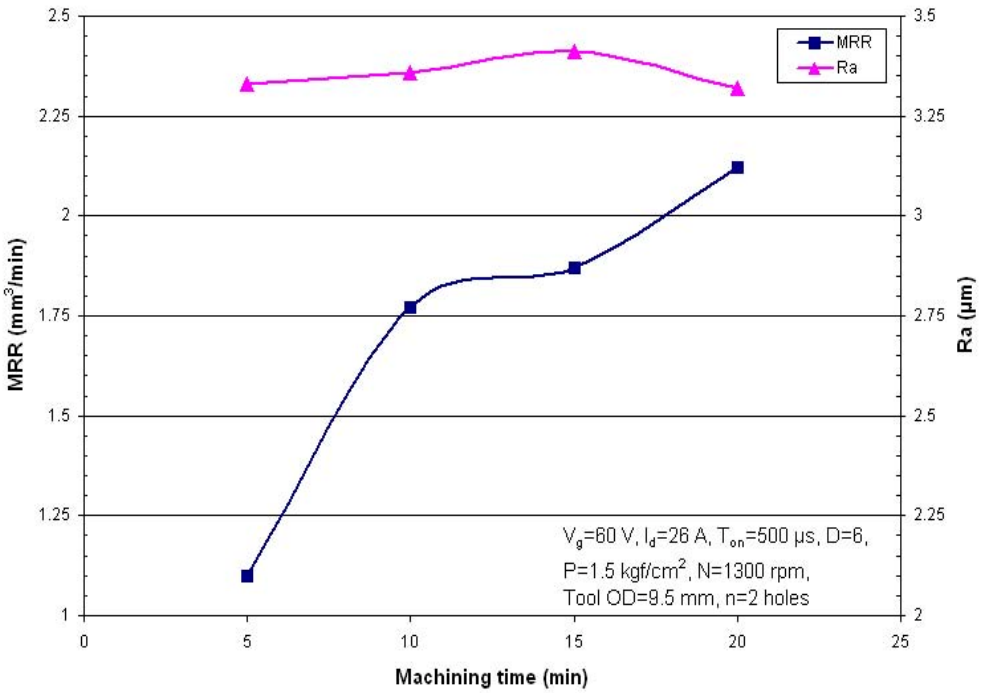

Figure 5.2: Variation of MRR (Material Removal Rate mm^3/min) with machining time

Based on the information derived from Figures 5.1 and 5.2, machining time for later stage experiments was set to 10 minutes. Each experiment was conducted for 10 minutes and the weight loss after machining was used to calculate the MRR.

5.2 One Variable at a Time (OVAT)

Effect of the input process parameters on the responses was studied by changing one parameter at a time while all others were held constant. One experiment was performed at each level of the parameter.

Effect of current

The effect of discharge current on MRR and Ra is shown in Figure 5.3. As expected, MRR was found to increase with an increase in the current. The spark energy increases with current which leads to higher crater volumes. Thus MRR increases with current. However, Ra values remain almost constant with increase in current. For higher currents, the crater volume may increase either due to an increase in the depth of the crater or the diameter of the crater or due to an increase in both of these. The Ra value is more sensitive to the crater depth as compared to the crater diameter. Hence, if with an increase in current, the size of crater is affected more than the depth of crater then the effect of increased current would not be observed clearly on the Ra values.

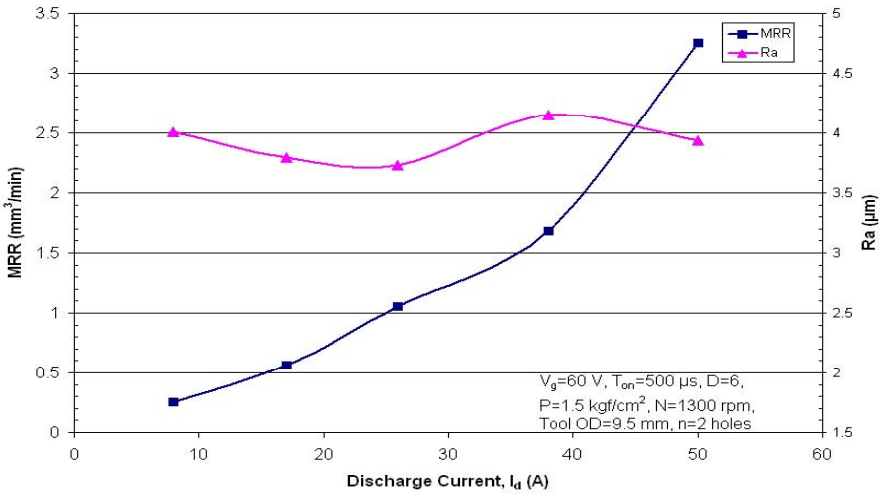

Figure 5.3: Effect of Discharge current on MRR (mm^3/min)

Effect of voltage

The effect of gap voltage on MRR and Ra is shown in Figure 5.4. Initially MRR increases with an increase in voltage but an optimum exists and the MRR drops with further increase in voltage. A similar trend was observed for Ra values which decrease up to an optimum point and then increase with voltage. Since spark energy is proportional to the gap voltage (Equation 2.2), increase in voltage would lead to a higher MRR. The decrease in Ra values with an increase in voltage suggests that larger but shallower craters are formed at higher voltage values. Discharge takes place when the effective electric field (=gap voltage/inter electrode distance) between the electrodes exceeds the dielectric strength of the medium. Hence, with an increase in the gap voltage the discharge gap distance increases and the breakdown electric field can now be achieved even at a larger gap distance. The effective gas velocity at the work piece surface is lower when the gap distance is high. Thus, flushing efficiency reduces and the probability of arcing increases due to the presence of debris in the tool-work piece gap. Due to partial removal of debris from the discharge gap, low MRR and a high Ra value was obtained at very high voltages. Thus an optimum value of voltage exists at which high MRR and low Ra value was obtained.

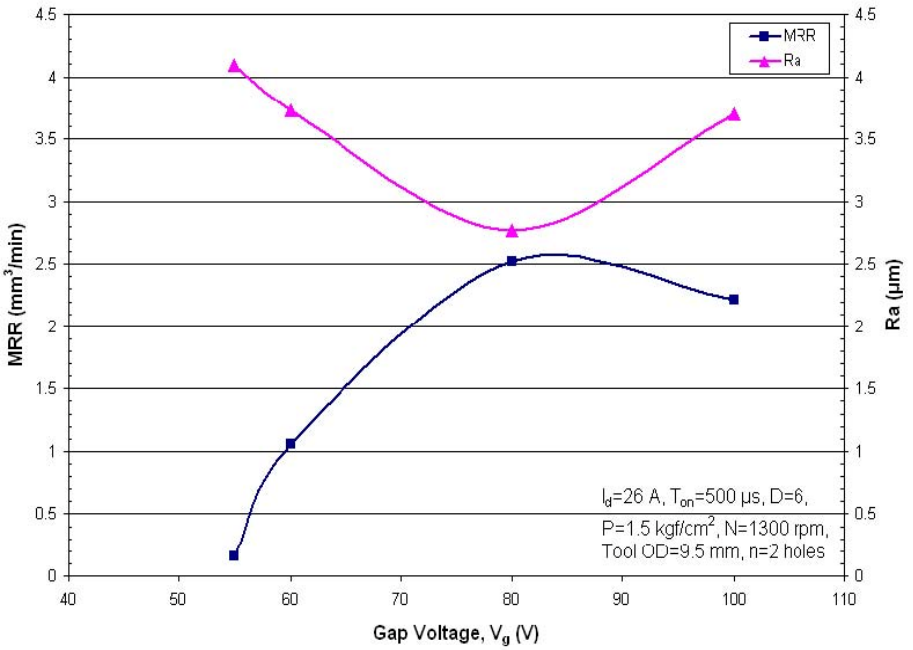

Figure 5.4 : Effect of Gap Voltage (Vg) on MRR (mm^3/min)

Effect of pulse-on time

The effect of pulse-on time on MRR and Ra is shown in Figure 5.5. It can be seen that MRR and Ra values both increase with an increase in the pulse-on time. The spark energy depends on T_{on} (Equation 3.2). For a higher T_{on}, the discharge crater is deeper and more material is removed per spark. This leads to higher Ra values. Also, Equation 3.3 for spark frequency may not hold true for a rotating tool as discussed in Section 3.3.1. Hence, in spite of a constant value of duty factor the MRR increases with T_{on}. For very large values of T_{on} the drop in MRR can be explained by the high values of pulse-off time. Since the duty factor was held constant during the experiment, a higher T_{off} value was obtained corresponding to a higher T_{on} value. No material removal occurs during the T_{off}. Hence, a high value of T_{off} increases non-cutting time and reduces the MRR. This non-cutting time however does not have a significant effect on the Ra value.

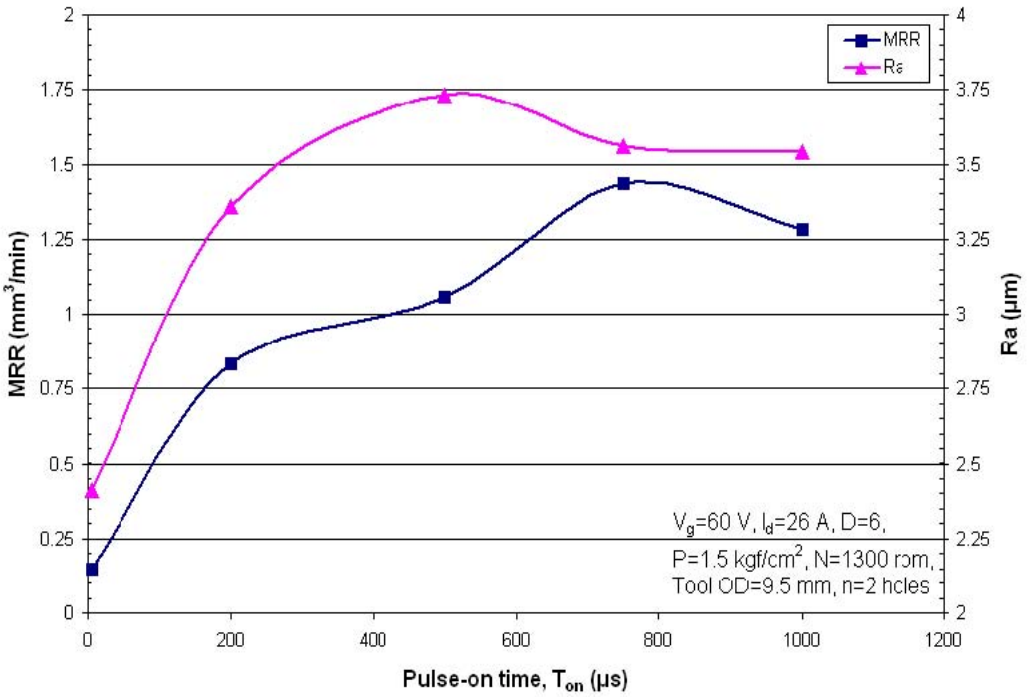

Figure 5.5: Effect of Pulse on time (Ton micro seconds) on MRR

Effect of pulse-off time

The effect of pulse-off time on MRR and Ra is shown in Figure 5.6. For a very small value of T_{off}, the MRR was low but then increased drastically when T_{off} was increased. The MRR then fell

slowly with an increase in T_{off}. For very short pulse-off time, the probability of arcing is high because the dielectric in the gap may not have completely recovered its dielectric strength. Also, the debris particles may still remain in the discharge gap. This would lead to a low MRR and high Ra value. When the T_{off} is sufficiently high, the dielectric regains its dielectric strength and the debris particles are also flushed away from the gap. Thus, a drastic increase in MRR and decrease in Ra value is achieved. With further increase in T_{off}, MRR decreased slowly because machining does not take place during the pulse-off time and it only adds to the non-cutting time. Further advantage due to dielectric strength recovery was not available hence increase in T_{off} leads to a decrease in MRR. The effect of increased T_{off} on Ra values cannot be explained by the above phenomenon as according to it the Ra values should have remained unaffected. One of the reasons for the observed trend in Ra values could be the effect of T_{off} on the re-solidification of molten work piece at the discharge crater. Molten material may re-solidify when long pulse-off times are used due to continuous supply of high velocity air through the tool. Also, air flow may distort the distribution of molten material in the crater leading to a poorer surface finish when the material solidifies. Further experiments are necessary to clarify this.

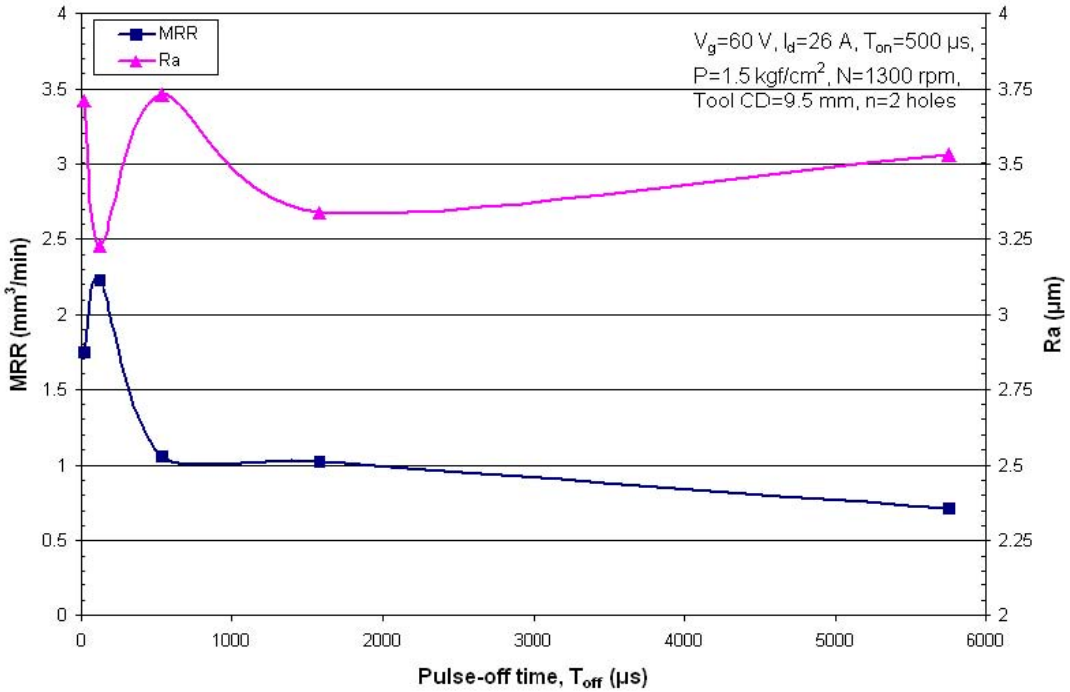

Figure 5.6: Effect of Pulse-off time on MRR

Effect of inlet air pressure

The effect of inlet air pressure on MRR and Ra is shown in Figure 5.7. The figure suggests that higher air pressure provides a better performance in terms of both the MRR and Ra values. Flushing efficiency improves with an increase in the pressure. A better removal of debris particles from the gap leads to a lower arcing probability. Arcing leads to surface damage, hence lower values of Ra were obtained with low arcing probability at high pressures. Also, when arcing is sensed by the EDM machine during a pulse, it stops power supply throughout the duration of the pulse. This increases the non-cutting time during machining leading to a lower MRR. Hence higher MRR was obtained at higher air inlet pressures.

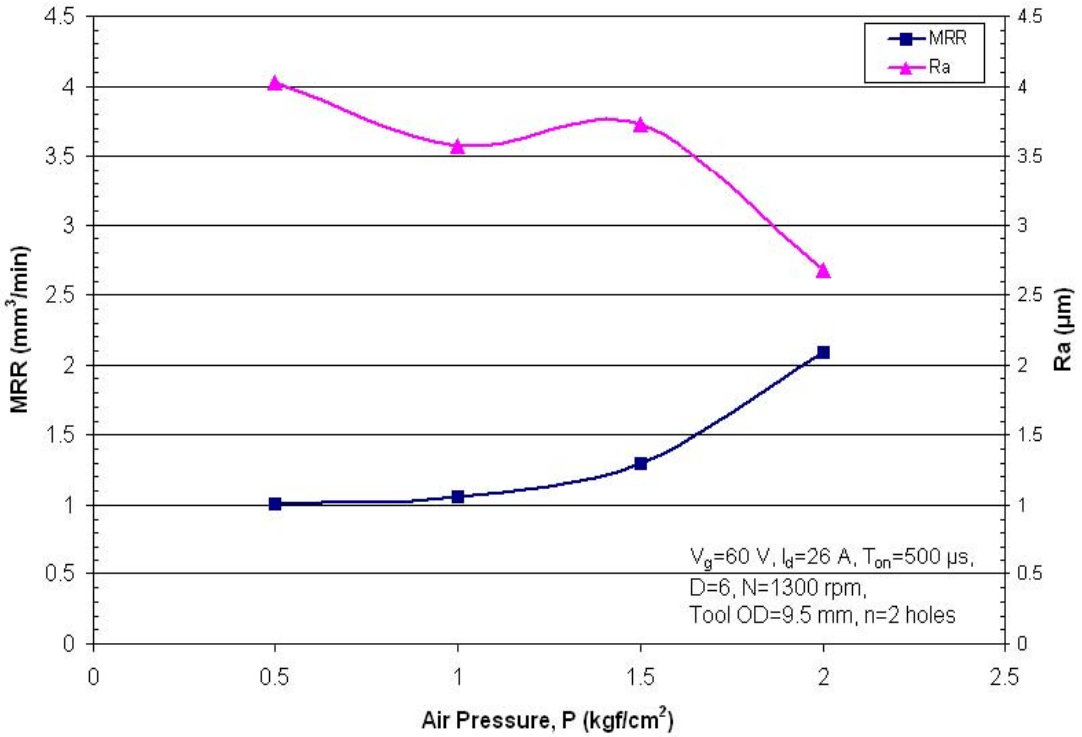

Figure 5.7: Effect of Air Pressure on MRR

Effect of spindle speed

The effect of spindle speed on MRR and Ra is shown in Figure 5.8. MRR initially increased with an increase in the spindle rpm but then saturated to a level and did not increase with an increase in the spindle rpm. Ra values also followed a similar trend and decreased with increase in spindle

rpm up to a level and then almost saturated. This behavior can be explained by the effect of spindle rotation on the discharge phenomenon. Spindle rotation during discharge leads to an improvement in the flushing efficiency. Due to rotation of the gas as it flows through the tube, the gas is forced outward away from the center when it comes out of the tool. This flow of gas takes the debris particles away from the discharge gap. The outward flow velocity of the gas is proportional to the spindle rotational speed and increases with it. This leads to an improvement in the flushing efficiency up to a maximum limit. After this stage, there is no scope for improvement in the flushing efficiency even on increasing the spindle speed since almost all the debris particles have been removed from the discharge gap. Hence, the MRR and Ra values saturated at very high values of the spindle speed. Apart from the flushing efficiency, tool rotation has an impact on the spark frequency. At high spindle speeds, a discharge may be interrupted even during the pulse-on time due to movement of the tool. Thus, several short sparks occur over a single pulse-on time and the spark frequency increases with the spindle rpm. Since the same pulse energy is now distributed over a number of sparks, the crater depth is lower. Hence, lower Ra values were observed when the spindle speed was increased.

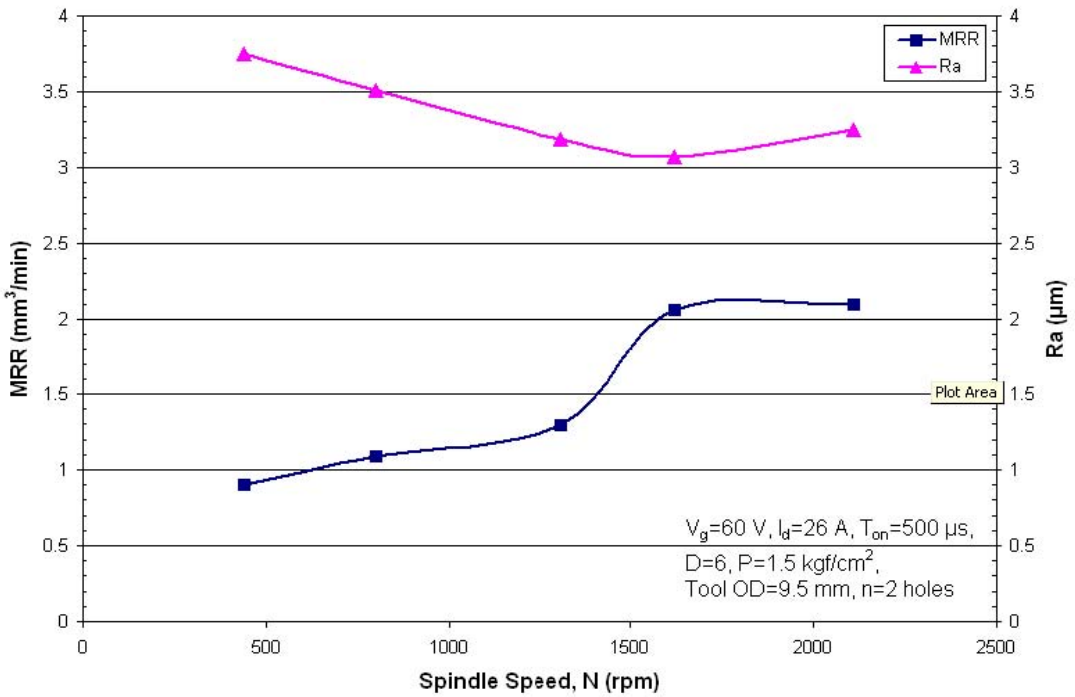

Figure 5.8: Effect of Spindle Speed on MRR

5.3 Parametric Analysis

In order to study the effect of the input parameters and the effect of their interactions, a designed experiment has been conducted. The OVAT analysis shows that effect of none of the factors is linear. Hence, a CCD design has been conducted which is capable of fitting a second order polynomial function.

CCD Observations

The experimental results obtained from the CCD runs are shown in Table 5.1. The runs were randomized and experiments were conducted in a single block. It is interesting to note that although the MRR and Ra values seem to change when the factors were changed, significant changes in TWR were not obtained. In most of the runs, the TWR in fact remained in the small range of [-0.02 0.02] mm^3/min.

Table 5.1: MRR, Ra and TWR observations of the CCD runs

Run Order	Input Parameters						Output Response		
	V_g	I_d	T_{on}	D	P	N	MRR	Ra	TWR
	V	A	µs		kgf/cm^2	rpm	mm^3/min	µm	mm^3/min
1	91	16	200	9	2.1	650	0.71	3.04	0.04
2	63	42	200	9	2.1	1900	5.68	3.14	-0.03
3	63	16	200	3	0.9	650	0.33	3.22	0.01
4	91	42	750	3	2.1	650	2.28	3.1	-0.02
5	91	16	200	9	0.9	650	0.55	3.46	-0.02
6	63	16	750	9	2.1	650	0.69	2.98	0.03
7	63	16	750	9	0.9	650	0.58	3.76	-0.06
8	77	29	500	11	1.5	1275	2.67	3.31	0.02
9	91	42	750	9	0.9	650	2.31	3.98	0.01
10	63	16	200	3	2.1	650	0.14	2.66	0.03
11	91	16	750	9	0.9	1900	1.03	3.25	-0.02
12	55	29	500	6	1.5	1275	0.87	3.53	0.02
13	77	29	500	6	1.5	1275	1.60	3.26	0.01
14	91	42	750	3	0.9	650	1.33	4.29	-0.01
15	63	16	200	3	0.9	1900	0.17	2.86	0.01

16	63	16	200	3	2.1	1900	0.68	2.4	-0.03
17	63	42	200	3	2.1	1900	2.31	2.46	-0.03
18	63	16	200	9	0.9	1900	0.99	2.96	0.03
19	91	16	200	3	2.1	650	0.47	2.63	0.04
20	63	42	200	3	0.9	1900	1.85	3.33	0.04
21	77	29	500	6	1.5	1275	1.58	3.25	0.01
22	63	42	750	9	2.1	1900	4.67	2.98	0.03
23	63	42	200	9	0.9	1900	5.37	3.11	0.02
24	91	42	200	9	0.9	650	3.19	4.27	0.03
25	77	49	500	6	1.5	1275	4.22	3.94	0.04
26	91	42	200	3	2.1	1900	2.44	3.5	0.02
27	91	16	200	3	0.9	650	0.26	3.42	0.01
28	91	16	200	3	0.9	1900	0.64	2.95	-0.02
29	63	42	750	3	2.1	1900	4.27	2.84	0.03
30	91	42	750	3	0.9	1900	2.86	4.08	0.01
31	77	29	50	6	1.5	1275	0.86	2.87	-0.01
32	63	16	200	9	0.9	650	0.36	3.36	0.02
33	91	16	750	3	2.1	650	0.53	3.01	0.02
34	91	42	750	3	2.1	1900	3.60	3.37	-0.02
35	77	29	500	6	0.6	1275	1.19	3.33	0.01
36	77	29	500	6	1.5	1275	1.82	3.21	0.04
37	63	16	200	9	2.1	650	0.47	2.86	-0.07
38	63	42	750	9	0.9	1900	3.31	4.2	0.04
39	63	42	200	9	2.1	650	4.67	3.3	-0.01
40	91	16	750	9	2.1	650	1.03	2.92	0.03
41	77	29	500	6	1.5	1275	2.04	3.35	-0.02
42	63	16	750	9	0.9	1900	0.88	3.7	0.07
43	77	29	1000	6	1.5	1275	2.69	3.13	0.02
44	77	29	500	6	1.5	2250	3.19	3.38	0.01
45	63	42	750	9	2.1	650	2.51	3.29	0.01
46	91	16	750	9	0.9	650	0.51	3.77	-0.02
47	91	42	200	3	0.9	650	1.22	3.4	0.02
48	91	16	750	3	0.9	1900	0.90	3.37	0.02
49	91	16	200	9	2.1	1900	1.14	2.48	0.02
50	63	16	750	3	0.9	650	0.49	3.78	0.02
51	77	29	500	6	1.5	1275	1.92	2.99	0.01
52	91	42	200	3	2.1	650	1.53	2.64	0.03
53	77	9	500	6	1.5	1275	0.51	2.85	0.03
54	77	29	500	6	1.5	1275	1.79	3.18	0.01
55	63	42	750	3	2.1	650	2.04	3.21	0.01
56	77	29	500	6	1.5	1275	1.79	3.3	0.02
57	91	42	200	9	2.1	650	2.69	3.57	0.04

58	77	29	500	6	1.5	1275	1.59	3.79	-0.01
59	91	16	750	3	0.9	650	0.55	3.68	0.02
60	63	42	750	3	0.9	650	1.55	3.89	-0.01
61	91	42	200	9	2.1	1900	4.19	3.34	0.02
62	63	42	750	9	0.9	650	1.94	4.28	0.01
63	77	29	500	6	1.5	1275	1.85	3.6	0.01
64	91	16	750	9	2.1	1900	1.06	3.1	-0.01
65	77	29	500	1	1.5	1275	1.10	3.49	0.03
66	91	42	750	9	0.9	1900	4.06	3.4	0.02
67	91	42	750	9	2.1	1900	4.42	3.28	0.01
68	63	42	200	3	2.1	650	1.81	3.6	0.03
69	99	29	500	6	1.5	1275	1.95	4.28	-0.03
70	91	42	750	9	2.1	650	2.88	3.65	-0.01
71	91	16	200	3	2.1	1900	0.68	2.49	0.02
72	77	29	500	6	2.5	1275	2.14	3.46	0.00
73	91	16	750	3	2.1	1900	0.51	2.75	0.00
74	77	29	500	6	1.5	1275	1.99	3	0.02
75	63	42	200	9	0.9	650	4.19	3.69	-0.03
76	63	42	200	3	0.9	650	1.21	3.07	0.02
77	91	16	200	9	0.9	1900	1.41	3.2	-0.02
78	77	29	500	6	1.5	300	1.00	3.49	0.01
79	63	42	750	3	0.9	1900	2.27	3.42	0.03
80	91	42	200	9	0.9	1900	4.19	3.81	0.01
81	63	16	750	3	2.1	1900	0.27	3.24	0.03
82	91	42	200	3	0.9	1900	1.81	3.08	0.00
83	63	16	750	3	0.9	1900	0.44	4.03	0.01
84	63	16	750	3	2.1	650	0.44	2.86	-0.02
85	63	16	200	9	2.1	1900	1.19	2.84	0.02
86	63	16	750	9	2.1	1900	0.79	3.5	0.01

5.4 Regression analysis and Model fitting

What is regression analysis?

Regression analysis gives information on the relationship between a response (dependent) variable and one or more (predictor) independent variables to the extent that information is contained in the data. The goal of regression analysis is to express the response variable as a function of the predictor variables. The duality of fit and the accuracy of conclusion depend on the data used. Hence non-representative or improperly compiled data result in poor fits and conclusions. Thus, for effective use of regression analysis one must

1. Investigate the data collection process,
2. Discover any limitations in data collected, and
3. Restrict conclusions accordingly.

Once a regression analysis relationship is obtained, it can be used to predict values of the response variable, identify variables that most affect the response, or verify hypothesized causal models of the response. The value of each predictor variable can be accessed through statistical tests on the estimated coefficients (multipliers) of the predictor variables.

An example of a regression model is the linear regression model which is a linear relationship between response variable, y and the predictor variable, $x_i, i = 1,2...,n$ of the form

$$y = \beta_0 + \beta_1 x_1 + \beta_2 x_2 + ... + \beta_n x_n + \varepsilon \quad (5.1)$$

where

$\beta_0, \beta_1 ..... \beta_n$ are regression coefficients (unknown model parameters), and

ε is the error due to variability in the observed responses.

Example 1

In the transformation of raw or uncooked potato to cooked potato, heat is applied for some specific tune. One might postulate that the amount of untransformed portion of the starch (y) inside the potato is a linear function of time (t) and temperature (θ) of cooking. This is represented as

$$y = \beta_0 + \beta_1 t + \beta_2 \theta + \varepsilon \quad (5.2)$$

Linear as used in linear regression refers to the form of occurrence of the unknown parameters, β_1 and β_2 as ,simple linear multipliers of the predictor variable. Thus, the two equations below are also both linear.

$$y = \beta_0 + \beta_1 t + \beta_2 t\theta + \beta_3 \theta + \varepsilon \quad (5.3)$$

$$y = \beta_0 + \beta_1 t\theta + \beta_2 \theta + \varepsilon \quad (5.4)$$

Comparison of Regression and Correlation

Unlike regression, correlation analysis assesses the simultaneous variability of a collection of variables. The relationship is not directional and interest is not on how some variables respond to

others but on how they are mutually associated. Thus, simultaneous variability of a collection of variables is referred to as correlation analysis.

Uses of Regression Analysis

Three uses for regression analysis are for

1. prediction
2. model specification and
3. parameter estimation.

Regression analysis equations are designed only to make predictions. Good predictions will not be possible if the model is not correctly specified and accuracy of the parameter not ensured. However, accurate prediction and model specification require that all relevant variables be accounted for in the data and the prediction equation be defined in the correct functional form for all predictor variables.

Parameter estimation is the most difficult to perform because not only is the model required to be correctly specified, the prediction must also be accurate and the data should allow for good estimation. For example, multi colinearity creates a problem and requires that some estimators may not be used. Thus, limitations of data and inability to measure all predictor variables relevant in a study restrict the use of prediction equations.

Multivariate Least Squares Fitting

Up until this point, we have considered single predictor variables in the specification of linear regression prediction equation. However, in most practical engineering problems, the independent variables or factors that determine or affect the dependent or the response variable are not often single predictor variables. If multiple independent variables affect the response variable, then the analysis calls for a model different from that used for the single predictor variable. In a situation where more than one independent factor (variable) affects the outcome of a process, a multiple regression model is used. This is referred to as multiple linear regression model or multivariate least squares fitting. Although flexibility is introduced into the regression analysis by the existence of multiple predictor variables, the complexity added by the use of multiple predictor variables makes this approach most suited for computer usage. A simple

example problem for which multiple predictor variables may be required is the consideration of factors on which the total miles traveled per gallon of gas by a car depends. Some of the factors that determine gas usage by a car include its speed, its weight and the wind conditions etc. Thus, for its analysis, a multiple regression model is used which is often referred to as multiple linear regression model or multivariate least squares fitting.

Unlike the single variable analysis, the interpretation of the output of a multivariate least squares fitting is made difficult by the involvement of several predictor variables. Hence, even if the data base is sound and correct model specified, it is not sufficient and correct to merely examine the magnitudes of the estimated coefficients in order to determine which predictor variables most affect the response. In the same vein, it is not sound to ignore the interactions of the predictor variables when considering the influence of any of the parameters. It is obvious from the fore going that modern day computer tools might have solved the computational aspect of the multivariate least squares method, but discerning the implications of the computational result remains a challenge.

The multivariate least squares discussion will be very brief. Consider N observations on a response y, with m regressors x_j, $j = 1,2,3,\ldots,m,$, the multiple linear regression model is written as

$$y_i = \beta_0 + \sum_{j=1}^{m} \beta_j x_{ij} \qquad i = 1,2,\ldots,N \tag{5.5}$$

In matrix form, we can arrange the data in the following form

$$X = \begin{bmatrix} 1 & x_{11} & x_{12} & \cdots & x_{1k} \\ 1 & x_{21} & x_{22} & \cdots & x_{2k} \\ \vdots & \vdots & & & \vdots \\ 1 & x_{N1} & x_{N2} & \cdots & x_{Nk} \end{bmatrix} \qquad Y = \begin{bmatrix} y_1 \\ y_2 \\ \vdots \\ y_N \end{bmatrix} \qquad \hat{\hat{a}} = \begin{bmatrix} \hat{\beta}_0 \\ \hat{\beta}_1 \\ \vdots \\ \hat{\beta}_k \end{bmatrix} \tag{5.6}$$

where $\hat{\beta}_j$ are the estimates of the regression coefficients, β_j which can be obtained from the solution of the matrix equation:

$$\hat{\hat{\alpha}} = \left(X'X\right)^{-1} X'Y \tag{5.7}$$

Equation 5.7 is obtained by setting up the sum of squares of the residuals and differentiating with respect to each of the unknown coefficients. Similar to the single variable regression, the

adequacy of the multiple least square regression models can be checked by computing the residuals and checking if they are normally distributed.

Above theoretical background it is clear that in present scenario we can apply multivariable linear regression analysis to estimate a model for three variables such as MRR, Ra and TWR.

Regression analysis of the experimental results obtained from the CCD runs has been done using MATLAB2010A mathematical tool.

Regression Analysis for MRR Variable

The final regression equation for MRR in terms of the actual parameter values is:

MRR_fit=MRR_a(1) + MRR_a(2).*Vg + MRR_a(3).*Id + MRR_a(4).*Ton + MRR_a(5).*D + MRR_a(6).*P + MRR_a(7).*N + MRR_a(8).*Vg.*Id + MRR_a(9).*Vg.*Ton + MRR_a(10).*Id.*D + MRR_a(11).*Id.*P + MRR_a(12).*Id.*N + MRR_a(13).*Ton.*D;

Where, MRR is in mm^3/min and Vg in V, Id in A, Ton in μs, D is dimensionless, P in kgf/cm^2, N in rpm, and MRR_a are coefficients determined from regression analysis.

Values of

MRR_a = [-1.05260.005460.0285-0.00043840.0688-0.2226-0.0002007-0.00066272.9096e-050.0080120.017262.9384e-05-0.000286]

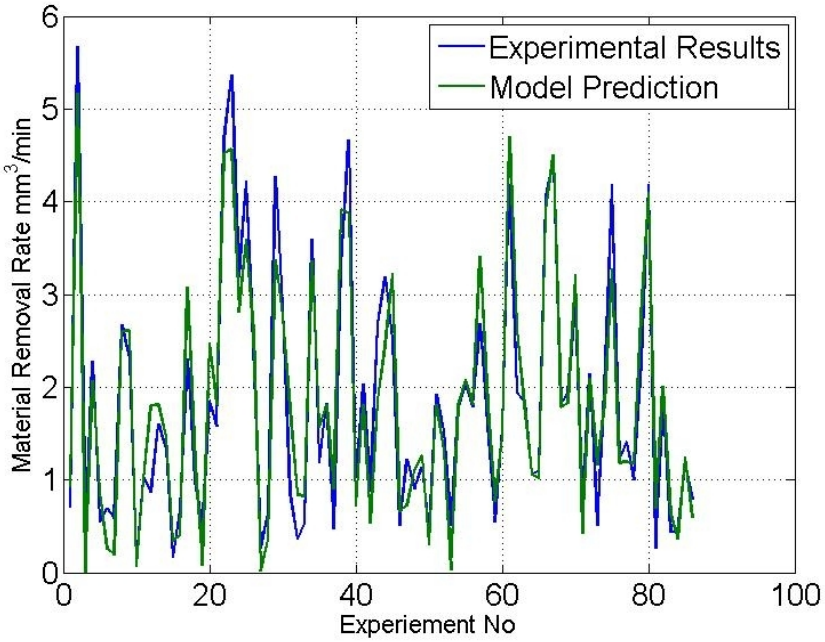

Figure 5.9: Comparisons of Experimental Results and Regression Analysis Results (MRR)

Regression Analysis for Ra

The final regression equation for Ra in terms of the actual parameter values is:

Ra_fit=Ra_a(1) + Ra_a(2).*Vg + Ra_a(3).*Id + Ra_a(4).*Ton + Ra_a(5).*D + Ra_a(6).*P + Ra_a(7).*N + Ra_a(8).*Vg.*Id + Ra_a(9).*Ton.*P + Ra_a(10).*Vg.^2 + Ra_a(11).*Ton.^2

(5.8)

Where, Ra is in μm and Vg in V, Id in A, Ton in μs, D is dimensionless, P in kgf/cm^2 and N in rpm, and Ra_a are coefficients of regression equation and estimated as below.

Ra_a= [7.9576 -0.1337-0.01620.00330.0265 -0.2064 -0.000147e-04 0.000381e-04 -0.00041e-04 0.000814e-04 -2.21787e-06]

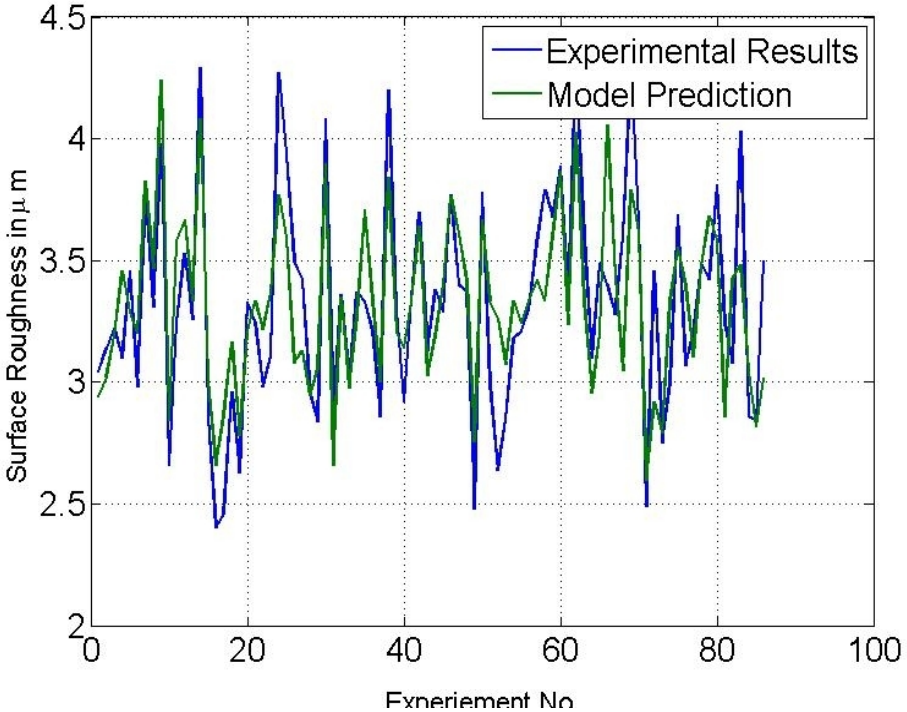

Figure 5.10 Comparisons of Experimental Results and Regression Analysis Results (Ra)

Regression Analysis for TWR

TWR_fit=TWR_a(1) + TWR_a(2).*Vg + TWR_a(3).*Id + TWR_a(4).*Ton + TWR_a(5).*D + TWR_a(6).*P + TWR_a(7).*N + TWR_a(8).*Vg.*Id + TWR_a(9).*Vg.*Ton + TWR_a(10).*Id.*D + TWR_a(11).*Id.*P + TWR_a(12).*Id.*N + TWR_a(13).*Ton.^D+ TWR_a(14).*Vg.^2 + TWR_a(15).*Id.^2; (5.9)

Where, TWR is in mm3/min and Vg in V, Id in A, Ton in μs, D is dimensionless, P in kgf/cm^2 and N in rpm, and TWR_a are coefficients of regression equation and estimated as below.

TWR_a=[0 0 0 0 0 0 0 0 0 0 0 0
4.10072238357340e-32 0 0]

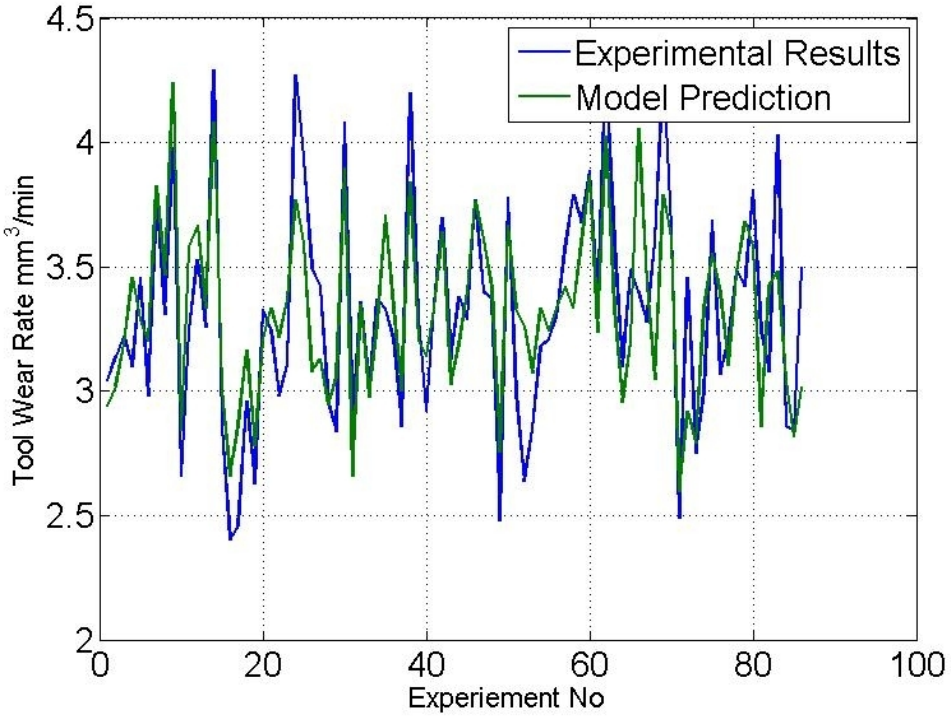

Figure 5.11: Comparisons of Experimental Results and Regression Analysis Results (TWR)

It is observed that three regression equations represented above have reasonable matching with experimental results. But in case of TWR regression an equation coefficient are erratic and gives less accurate prediction as compared to other regression equation.

5.5 Response surface analysis

MRR Response Surface

The response surfaces of MRR were obtained for the interaction terms in the reduced two-factor interaction model. Response surface of MRR versus gap voltage and discharge current is shown in Figure 5.12. From the figure it can be seen that a high current and voltage combination leads to high MRR due to an increase in the spark energy as given by Equation 3.4. It can be observed from the figure that at low current values, MRR increases with an increase in voltage due to increase in the spark energy. However, at high current levels, an increase in voltage leads to a slight decrease in the MRR. One of the reasons for this could be the higher amount of debris formation and higher flushing required at high current levels. Since, discharge gap increases with

an increase in voltage; flushing efficiency is reduced at high voltages. The increase in spark energy is dominated by the reduction in spark efficiency as voltage is increased. This leads to a reduction in MRR as voltage is increased at high current levels. The response surface of MRR versus gap voltage and pulse-on time is shown in Figure 5.12. From the figure it can be seen that the effect of Vg and T_{on} is not significant and the MRR values remain almost constant with changes in Vg and Ton.

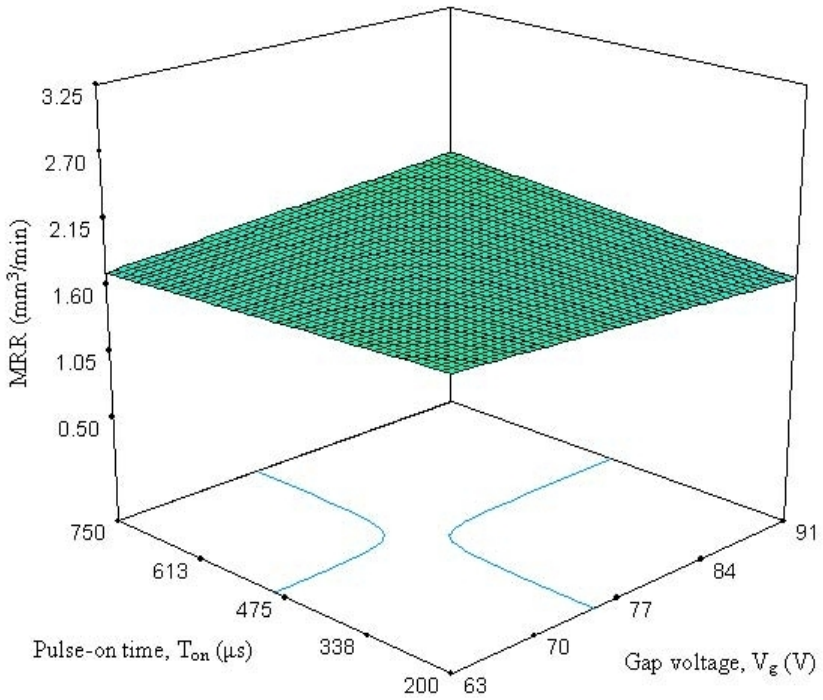

Figure 5.12: Effects of Gap Voltage and Discharge Current on MRR

Response surface of MRR versus discharge current and duty factor setting is shown in Figure 5.13. From the figure it can be observed that MRR increases with an increase in duty factor and current in accordance with Equation 3.4. Similarly, from Figure 5.14 and Figure 5.15 it can be observed that high MRR is obtained at high current and high air inlet pressure combination and high current and high spindle speed combination. High values of air pressure and spindle speed lead to a better flushing efficiency which improves the MRR. MRR increases on increasing any of the five factors (Vg, Id, D, P, N), but it can be seen Id has the highest effect on MRR.

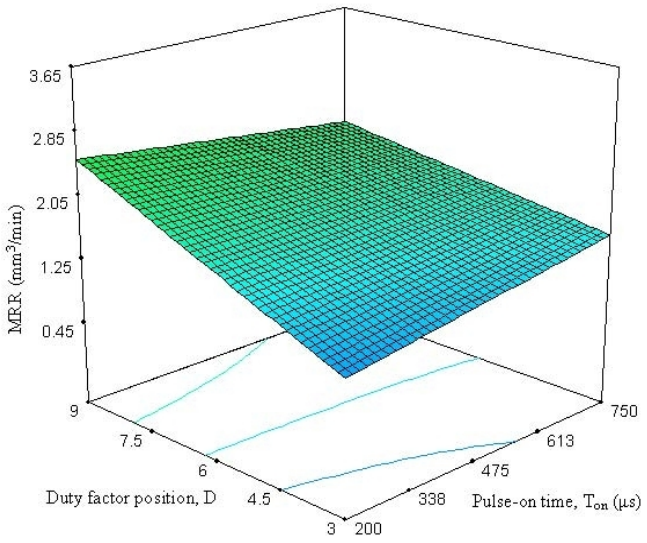

Figure 5.13: Effects of Gap Voltage and Pulse on Time on MRR

The effect of pulse-on time is not straightforward as can be seen from the response surface of MRR versus T_{on} and D (Figure 5.13). For high values of duty factor, an increase in T_{on} leads to a decrease in the MRR where as for low values of duty factor, an increase in T_{on} leads to an increase in MRR. A possible reason for this could be that for high duty factors, the pulse-off time is low. When a high T_{on} is used, the amount of material which melts during the spark increases due to higher spark energy. However, due to extremely low pulse-off times, a substantial part of the material re-solidifies or remains in the spark gap instead of being flushed away from the gap. With an increase in T_{on}, the amount of debris particles in the spark gap is expected to increase. This leads to a higher arcing probability and reduces the MRR. On the other hand, high pulse-off time is obtained at low duty factor and sufficient time for flushing of debris from the gap is available in between the sparks. Hence, when a high T_{on} is used more material is melted and the material is also removed due to flushing. Thus MRR increases on increasing Ton at low duty factors.

Discharge Current on MRR

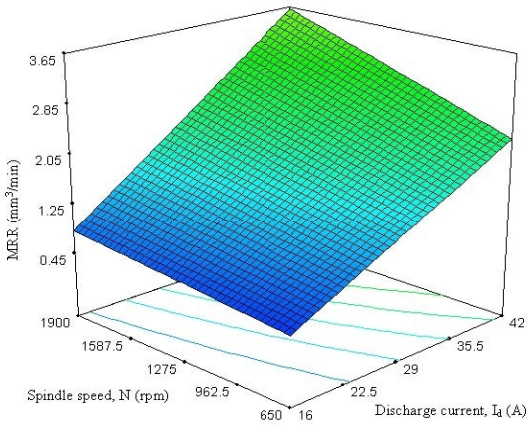

Figure 5.14: Effects of Spindle Speed and Discharge Current on MRR

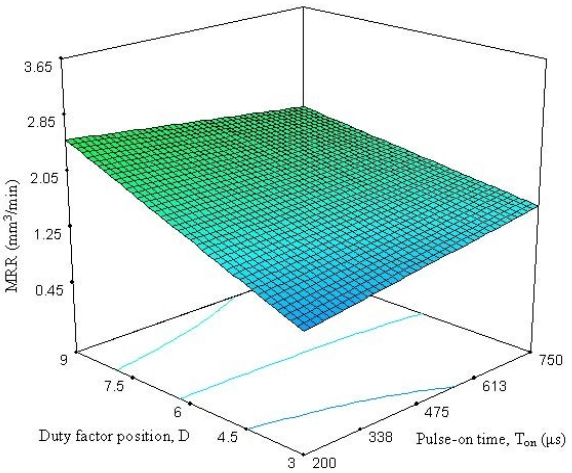

Figure 5.15: Effects of Pulse on time and Duty factor Position on MRR

Ra Response Surface

The response surfaces of Ra were obtained for the interaction terms in the reduced quadratic model. Response surface of Ra versus gap voltage and discharge current is shown in Figure 5.17. From the Vg-Id response surface it can be seen that the Ra value decreases with a decrease in the current. However, an optimum exists for voltage. Also, this optimum point depends on the value of the current. The existence of optimum voltage can be explained as in the case of OVAT analysis. The optimum voltage shifts towards higher values as the current decreases. At low currents, the amount of debris formed is lower because of the lower spark energy. Thus the need for flushing is not as significant at lower currents as in the case of higher currents. At lower voltage values the flushing efficiency is reduced due to lower spark gap. Hence for obtaining the same Ra value at higher current levels, lower voltage values are required. Thus, the optimum voltage value decreases with an increase in the current value. Response surface of Ra versus pulse-on time and air inlet pressure is shown in Figure 5.18. Corresponding to every air pressure, a Ton value exists at which the Ra value is highest and Ra decreases on either side of this Ton value. For very low values of Ton, high frequency sparks take place leading to shallower crater formation. This leads to a low Ra value for very low Ton values. But for very large values of Ton,

the T_{off} values also increase (since the duty factor is held constant). Thus, flushing efficiency improves leading to a lower Ra value. The Ton corresponding to highest Ra value depends on the value of air pressure. High values of Ton lead to melting of more material per spark requiring better flushing. Thus at high pressure values (i.e. better flushing conditions), higher Ton values can be afforded for the same Ra value (as seen on the contour plot in Figure 5.18). The duty factor does not show interaction effect with any other factor. The effect of duty factor can be seen from the regression equation 5.2. Ra values increase on increasing the duty factor. High duty factors lead to more material removal and higher debris formation. This increases the arcing probability and leads to poorer surface finish.

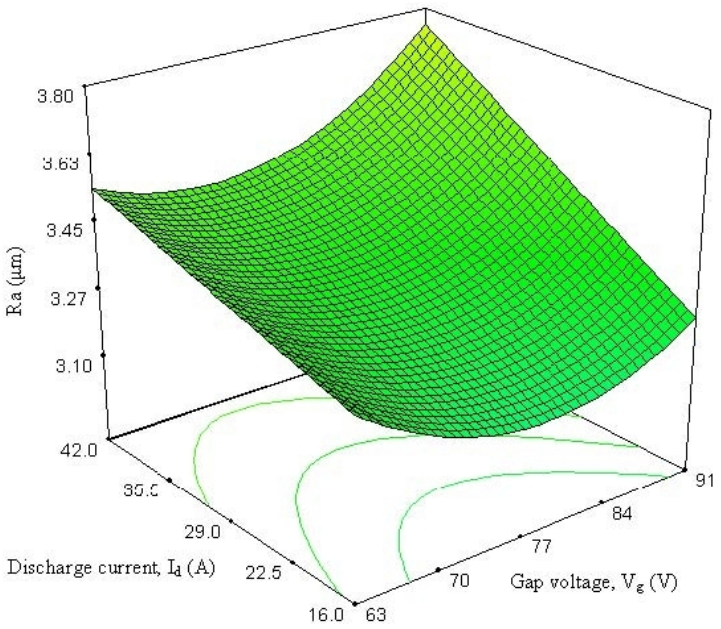

Figure 5.17: Effects of Gap Voltage and Discharge Current on Ra

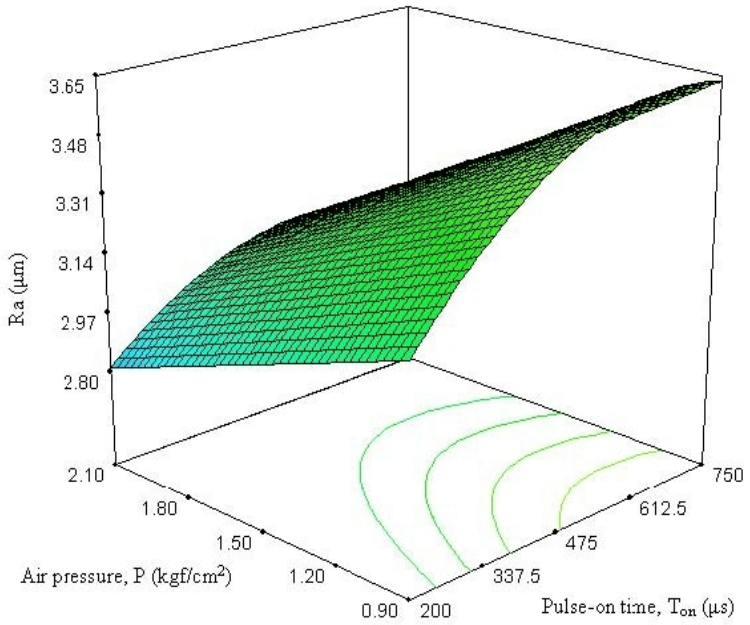

Figure 5.18: Effects of Pulse on time and Air Pressure on Ra

CHAPTER 6

CONCLUSION

In the present work, parametric analysis of the dry EDM process has been done based on experimental results. Experiments based on the Central Composite Design (CCD) were conducted to develop empirical models of the process. Following conclusions can be drawn from the analysis of the results:

- ✓ From the preliminary experiments it was found that EDM with air as the dielectric is feasible with reverse polarity. However, high velocity gas flow into the inter-electrode gap through a hollow tubular tool electrode and rotation of the tool are necessary conditions for obtaining a reasonable material removal rate. Flow characteristic of the gas in the inter-electrode gap affects the material removal rate (MRR) and the surface roughness (Ra), as

was observed on changing the tool outer diameter and the number of air-flow holes in the tool.

- ✓ From the designed set of experiments based on CCD it was found that discharge current, duty factor, air pressure and spindle speed are the significant factors which affect MRR and MRR increases with an increase in any of these factors. For MRR, most significant two-factor interaction effects are present among current and duty factor, current and spindle speed and pulse-on time and duty factor.

- ✓ From CCD experiments it was found that except for gap voltage all other input parameters (discharge current, pulse-on time, duty factor, air pressure and spindle speed) have significant effect on Ra. Ra values decrease with a decrease in the values of current and duty factor. Also, Ra values decrease with an increase in the values of air pressure and spindle speed. No significant two-factor interactions were found for Ra. However, Ra was found to have a quadratic dependence on gap voltage and pulse-on time.

- ✓ Based on the CCD experiments, the tool wear rate (TWR) was found to be very small (less than 1% of the MRR). It was found that the TWR is independent of the input parameters.

- ✓ Multi-objective optimization revealed that high air pressure and high spindle speed combination is favorable for obtaining both a high MRR and a low Ra. Such a combination of these input parameters leads to a higher flushing efficiency. Rough machining region (high MRR) was obtained for high current, low pulse-on time and high duty factor values. Finish machining region (low Ra) was obtained for low current, high pulse-on time and low duty factor values.

- ✓ Focused experiments conducted in the finish and rough machining regions revealed the existence of an additional process constraint based on the flushing efficiency. Flushing efficiency cannot increase indefinitely with an increase in air pressure and spindle speed since it saturates (theoretically to 100%) beyond some combination of air pressure and spindle speed.

- ✓ The air pressure and spindle speed values for flushing efficiency saturation depend on the amount of debris produced during machining and hence depend on the MRR. Under high MRR conditions, higher pressure and spindle speed values are required for obtaining the saturation point of flushing efficiency. Thus, predictions of the optimization model presented here are more close to the experimental values in the rough machining region than in the finishing region.

- ✓ A comparison of the process performance of dry EDM and oil EDM shows that a better surface finish is obtained in dry EDM for comparable values of MRR. Additionally, the TWR in dry EDM is very low. This suggests that the dry EDM process is more suitable for precision EDM operations.

CHAPTER 7

SCOPE FOR FUTURE WORK

Analysis of the results obtained from the current work suggests several feasible extensions to the research. Some of them are listed below:

- ✓ One of the most relevant extensions would be conducting further experimental investigations to identify the practical constraints (such as flushing efficiency) as a function of the input parameters in order to improve the empirical process models and the process optimization. Apart from that, the current research establishes fairly well that the material removal rate (MRR) in dry EDM with air as dielectric is poorer than oil EDM; however the tool wear rate (TWR) and surface finish are better. Hence, further work may focus more on developing dry EDM as a precision machining process. For that, it is important to study not only the surface finish but also other performance variables such as over-cut, process repeatability and surface integrity.

- ✓ The current work was done using air as dielectric. It would be interesting to compare the process performance of other gaseous dielectrics. Oxygen, nitrogen, helium and argon are some of the most promising ones. It is expected that high MRR would be obtained with oxygen. Nitrogen may be helpful if surface treatments such as nitriding are required post-machining. Helium has a relatively very high heat capacity and may provide better performance in terms of precision of the cut. An optimization similar to the one presented in this work may be performed and Pareto-fronts from each dielectric may then be superimposed on the same graph. That would help in selecting the best dielectric-parameter setting combination for the finish and rough machining conditions. The performance of various gas-liquid dielectric combinations in near-dry EDM may also be studied.

- ✓ In terms of applications, the dry EDM process may be implemented for micromachining. Not much work has been done in this field so far and it would require building up a knowledge base for the process at the micro-level to make dry Electric Discharge Micromachining feasible. Additionally, dry EDM milling characteristics may be

investigated by implementing X-Y table movement. Complex two or two and a half dimensional parts may be machined using the dry EDM milling process.

- ✓ Apart from experimental work, ample scope exists for theoretical modeling and process simulation (such as finite element analysis) in dry EDM. Current literature is insufficient in this regard. Existing oil EDM theory and simulation models may be modified to include the effect of the gaseous dielectric. Also, further computational work is required to fully understand the fluid dynamics of the dielectric gas flow in the inter-electrode gap and its effect on process performance. Results from the developed theoretical and computational models may then be compared with the experimental results reported in this work.

REFERENCES

[1] Leão, F.N., Pashby, I.R. A review on the use of environmentally-friendly dielectric fluids in electrical discharge machining (2004) Journal of Materials Processing Technology 149 (1-3), pp. 341-346.

[2] Ramani, V., Cassidenti, M. L., Inert-Gas Electrical Discharge Machining (1985) NASA, National Technology Transfer Center (NTTC), Wheeling, WV.

[3] M. Kunieda, S. Furuoya and N. Taniguchi, Improvement of EDM efficiency by supplying oxygen gas into gap (1991) CIRP Annals-Manufacturing Technology 40, pp. 215-218.

[4] M. Kunieda, M. Yoshida and N. Taniguchi, Electrical discharge machining in gas, (1997) CIRP Annals-Manufacturing Technology 46, pp. 143-146.

[5] M. Kunieda, Y. Miyoshi, T. Takaya, N. Nakajima, Y.Z. Bo and M. Yoshida, High speed 3D milling by dry EDM (2003) CIRP Annals-Manufacturing Technology 52, pp. 147-150.

[6] Yu, Z., T. Jun, and K. Masanori, Dry electrical discharge machining of cemented carbide (2004) Journal of Materials Processing Technology, 14th International Symposium on Electromachining (ISEM XIV) 149 (1-3) pp. 353-357.

[7] Kunieda, M., Takaya, T., Nakano, S. Improvement of dry EDM characteristics using piezoelectric actuator (2004) CIRP Annals - Manufacturing Technology 53 (1), pp. 183-186.

[8] Y. Zhanbo, J. Takahashi, N. Nakajima, S. Sano, K. Karato, M. Kunieda, Feasibility of 3-D surface machining by dry EDM (2005) International Journal of Electrical Machining10, pp.15-20.

[9] Zhang, Q.H., Zhang, J.H., Ren, S.F., Deng, J.X., Ai, X. Study on technology of ultrasonic vibration aided electrical discharge machining in gas (2004) Journal of Materials Processing Technology, 14th International Symposium on Electromachining (ISEM XIV) 149 (1-3), pp. 640-644.

[10] Zhang, Q.H., Du, R., Zhang, J.H., Zhang, Q.B. An investigation of ultrasonic-assisted electrical discharge machining in gas (2006) International Journal of Machine Tools and Manufacture 46 (12-13), pp. 1582-1588.

[11] Kunieda, M., Furudate, C. High precision finish cutting by dry WEDM (2001) CIRP Annals - Manufacturing Technology 50 (1), pp. 121-124.

[12] Kao, C.C., Tao, J., Lee, S., Shih, A.J. Dry wire electrical discharge machining of thin workpiece (2006) Transactions of the North American Manufacturing Research Institute of SME 34, pp. 253-260.

[13] Jia Tao, Albert J. Shih, and Jun Ni, Experimental Study of the Dry and Near-Dry Electrical Discharge Milling Processes (2008) Journal of Manufacturing Science and Engineering 130, 011002, DOI:10.1115/1.2784276

[14] J.S. Soni, G. Chakraverti, Machining characteristics of titanium with rotary electro-discharge machining (1994) Wear 171, pp.51-58.

[15] Schumacher, B.M. After 60 years of EDM the discharge process remains still disputed (2004) Journal of Materials Processing Technology 149 (1-3), pp. 376-381.

[16] Jiju Anthony. Design of experiments for engineers and scientist (2003) Butterworth-Heinemann, ISBN0 7506 4709 4.

[17] Myers, R. H. and D. C. Montgomery. Response surface methodology: process and product optimization using designed experiments, Second edition (2002) Wiley, New York

[18] K. Deb and R. B. Agrawal. Simulated binary crossover for continuous search space (1995) Complex Systems 9, pp.115-148.

[19] K. Deb, An efficient constraint handling method for genetic algorithms (2000) Computational Methods in Applied Mechanical Engineering 186, pp. 311–388.

[20] Deb, K., Pratap, A., Agarwal, S., Meyarivan, T. A fast and elitist multi objective genetic algorithm: NSGA-II (2002) IEEE Transactions on Evolutionary Computation 6 (2), pp. 182-197.

[21] Les Horve, Shaft Seals for Dynamic Applications (1996) Marcell Dekker (Hardcover)

[22] Prof. Kalyanmoy Deb's KANGAL Research Group at IIT Kanpur, http://www.iitk.ac.in/kangal/index.shtml